Interactive effects of abiotic factors and biotic agents on Scots pine dieback: A multivariate modeling approach in southeast France

Jean Lemaire, Michel Vennetier, Bernard Prévosto, Maxime Cailleret

Interactive effects of abiotic factors and biotic agents on Scots pine dieback : A multivariate modeling approach in southeast France.

Jean Lemaire[1], Michel Vennetier[2], Bernard Prévosto[2], Maxime Cailleret[2],

Abstract

Forest dieback is a high risk factor for the sustainability of these ecosystems in the climate change context. Productivity losses and increased defoliation and mortality rates have already been recorded for many tree species worldwide. However, dieback is a process that depends on complex interactions between many biotic and environmental factors acting at different scales, and is thus difficult to address and predict.

Our aim was to build tree- and stand-level foliar deficit models integrating biotic and abiotic factors for Scots pine *(Pinus sylvestris),* a species particularly threatened in Europe, and especially in the southeastern part of France. To this end, we quantified foliar deficit in 1740 trees from 87 plots distributed along an environmental gradient. We also measured tree annual radial growth and the abundance of two parasites: the pine processionary moth (*Thaumetopoea pityocampa* Den. & Schiff.) and mistletoe *(Viscum album* L.*)*. Topographic, soil, climate and water balance indices were assessed for each plot, together with the stand dendrometric characteristics. Given the large number of environmental factors and the strong correlations between many of them, models were developed using a partial least squares (PLS) regression approach.

All the models pointed to a preponderance of the biotic factors (processionary moth and mistletoe) in explaining the intensity of foliar deficit at both tree- and stand- levels. We also show that strong interactions between climate, soil, water balance and biotic factors help to explain the intensity of dieback. Dieback was thus greater in the driest topoedaphic and climatic conditions where the mistletoe and processionary moth were present.

This study highlights the need to account for a wide range of biotic and abiotic factors to explain the complex process of forest dieback, and especially the environmental variables that contribute to the water balance on the local scale. The phenomenological modeling approach presented here can be used in other regions and for other species, after a re-calibration and some adaptations to local constraints considering the limited distribution area of some biotic agents.

[1]**Jean Lemaire : Centre National de la Propriété Forestière, Institut pour le Développement Forestier. Aix-Marseille université jean.lemaire@cnpf.fr 175 cours Lafayette. F-69006 LYON**

[2] **Michel Vennetier michel.vennetier@inrae.fr, Bernard Prévosto bernard.prevosto@inrae.fr and Maxime Cailleret maxime.cailleret@inrae.fr. INRAE, Aix-Marseille University.**
UMR RECOVER. 3275 route de Cézanne CS 40061 F- 13182 Aix-en-Provence Cedex 5.

1. Introduction

Ever since the beginning of the industrial era in the 19th century, human activities have been associated with a significant rise in global temperatures, forecast to continue in the range of +1°C to +5.7 °C by 2100 according to climate scenarios (relative to the period 1850-1900 ; Masson-Delmotte *et al*., 2021). This gradual temperature rise has been accompanied by an increased frequency and intensity of extreme weather events and summer droughts in some regions, such as the Mediterranean (Cramer *et al*., 2018). These climate changes intensify the physiological stress undergone by forest ecosystems, leading to short- and long-term modifications in their carbon and water economies (McDowell *et al*., 2008), and in their structure and composition (Anderegg *et al*., 2013).

One sign of these dysfunctions at both tree and stand levels is dieback, defined as weakened vitality of a tree relative to a healthy reference tree, or weakened vitality of a large number of trees in a stand (Schütt and Cowling, 1985). Visible clues of dieback include reduced radial growth (Helama *et al*. 2014; Camarero *et al*. 2018), changes in crown architecture, branch and root death, fewer or smaller seeds (Girard *et al*., 2012; Vennetier *et al*., 2013), and most often a leaf area deficit (Becker *et al*., 1990; Carnicer *et al*., 2011; Dobbertin and Brang, 2001). Dieback may degenerate in tree death in the absence of recovery (Bréda *et al*., 2006). Besides these visible clues, various physiological and anatomic signs can be reported, including changes in carbon reserves (Adams et al., 2013), lower efficiency in the use of resources (Gessler *et al*., 2018), xylem embolism (Choat *et al*., 2012), or nutrient imbalance (Gessler *et al*., 2017). Mechanistically, dieback is described as a complex system in which various biotic and abiotic factors interact in chains (Franklin *et al*., 1987; Waring, 1987). Commonly cited biotic factors include fungi, insects, bacteria, plant parasites, and inter-tree competition. Abiotic factors are related to climate, topography, soil, and sometimes air pollution. Dieback processes are often triggered by weather events, in particular severe droughts (Bigler *et al*., 2006; Suarez *et al*., 2004; Das

et al., 2007; Pedersen, 1998; Gaylord *et al*., 2015), which are increasingly associated with heatwaves (Teskey *et al*., 2015; Vogel *et al*., 2021). These factors can be compounded with spells of deep frost, either early or late, but also with biotic agent outbreaks (e.g., Morcillo *et al*., 2019).

Forest dieback affects many biomes and species worldwide (e.g., van Mantgem *et al*. 2009; Allen *et al*., 2010; Hartmann *et al*., 2018; Hartmann *et al*. 2022), including Scots pine *(Pinus sylvestris),* a main European tree species that covers more than 20 million hectares from Scandinavia to southern Spain (Gonthier *et al*. 2011; Houston Durrant *et al*. 2016). It is particularly impacted in the southern part of its distribution range, in the Pyrenees and the Alps, but also in central Europe. These dieback events are often attributed to drought (e.g., Bigler *et al*. 2006; Bose *et al*. 2020; Buras *et al*. 2018; Camarero *et al*. 2015; Etzold *et al*. 2019; Martínez-Vilalta *et al*. 2009), but it also involves biotic factors such as the pine processionary moth (*Thaumetopoea pityocampa* Den. & Schiff.) (Hódar *et al*., 2003), and mistletoe (*Viscum album* L.) a hemiparasitic plant that causes gradual weakening of infested trees (Dobbertin *et al*. 2005; Galiano *et al*. 2010; Rigling *et al*. 2010 ; Kollas *et al*. 2018).

Determining the potential interactions between stand attributes, climate, processionary moth and mistletoe in the dieback process is key with regard to climate change. When water and nutrients availability are not limited, pine mistletoes can co-exist with their host tree for years (Solomon *et al.*, 2015; Zuber, 2004). However, during drought, mistletoes maintain high transpiration rates (Zweifel *et al*., 2012), which may exacerbate the stress experienced by the host pine, with negative consequences on the growth performance and on foliar deficit (Dobbertin and Rigling, 2006; Rigling *et al*., 2010; Wang *et al*., 2022). Considering that epidemic phases of the processionary moth can also cause strong pine defoliation, and that both biotic factors are favoured by sunny and warm positions, and thus

potentially by transparent canopies, synergies between these factors, drought, and the microenvironment are likely (e.g,. Gea-Izquierdo *et al*., 2019).

Both biotic factors are favored by higher temperature, and upward or northward shifts have been reported in several areas (e.g., Dobbertin *et al.* 2005; Robinet *et al.* 2007 and 2014). However, quantification of this process requires long-term data series, which are rarely available and may show a different trend (e.g., Camarero *et al.,* 2022 in the case of processionary moth).

In the last 20 years, many numeric models have been developed to predict the endpoint of dieback, namely tree death. On the one side, physiological models explicitly simulate the carbon and hydraulic mechanisms involved in tree death (e.g., McDowell *et al*., 2013; Cochard, 2020; Davi and Cailleret, 2017). On the other side, phenomenological models predict mortality risk using statistical approaches based on local abiotic environmental data (soil, climate, topography) and dendrometric data (type of stand, density, tree size, etc.) without considering the physical and physiological mechanisms behind tree dieback (e.g., Taccoen *et al*., 2019). Along this continuum are models that couple empirical and mechanistic approaches (e.g., Venturas *et al*. 2021), and others that use integrative indicators of tree vitality, such as radial growth (e.g., Bigler and Bugmann, 2004; Holzwarth *et al*., 2013; Hülsmann *et al*., 2018). Physiological models are considered as more accurate in the context of a changing environment, but they require a large amount and diversity of high-resolution data, and are not yet fully functional for many species and over large areas. Phenomenological models are more parsimonious and robust within their calibration range, but less reliable outside it. Despite the increasing number, diversity and complexity of models that predict whether a tree will live or die, prediction of mortality at a regional scale is still challenging (Trugman *et al*., 2021), and few models simulate a tree's level of dieback, owing to lack of data and because dieback displays a wide range of signs. These dieback models, for example those that predict foliar deficit (e.g., Galiano *et al*., 2010; Gonthier *et*

al., 2011), cannot be used directly for forestry diagnostics as they consider only a few factors influencing tree health, either directly or indirectly (through their interactions), and often neglect site factors (e.g., soil and topography). However, in view of the current increase in forest dieback at both local and global scales, operational tools able to predict this risk are urgently needed.

The aim of this study was to partly fill this research gap by developing phenomenological models to predict foliar deficit of Scots pine. We used a partial least squares (PLS) regression approach to (1) assess the impact of multiple environmental factors (climate, soil, topography) and of the spatial distribution of pine populations at landscape scale on the abundance of biotic agents : pine processionary moth and mistletoe; (2) disentangle the respective and interactive impacts of these abiotic and biotic drivers on foliar deficit on both tree and stand scales; and (3) develop a model that could be used by forest managers to predict the risk of stand dieback. With this multifactorial and multiscale approach, we aimed at improving our understanding of the dieback process on Scots pine and the methodologies used to predict dieback risk.

2. Materials and Methods

2.1 Study area

The study was conducted in southeast France (Figure 1), where Scots pine is the main forest species in terms of area and timber volume. This pioneering species has naturally recolonized a large part of the agricultural land that has been abandoned in the last 150 years, and has also been planted to protect the soil in mountain areas (Médail, 2001). Scots pine is moderately tolerant of both drought and cold, and not markedly sensitive to pH or soil type. It was thus present in our study area in different biomes over a broad range of climatic conditions, from a typical Mediterranean climate, alongside downy oak (*Quercus pubescens* Willd.), to a mountain climate with common beech (*Fagus sylvatica* L.) and silver fir (*Abies alba* Mill.) (Le Houerou, 2005; Joly *et al*., 2010). Scots pine dieback has

been a major concern for the past 30 years in this area (Pauly and Belrose, 2005; Sardin, 1997; Thabeet *et al*., 2009).

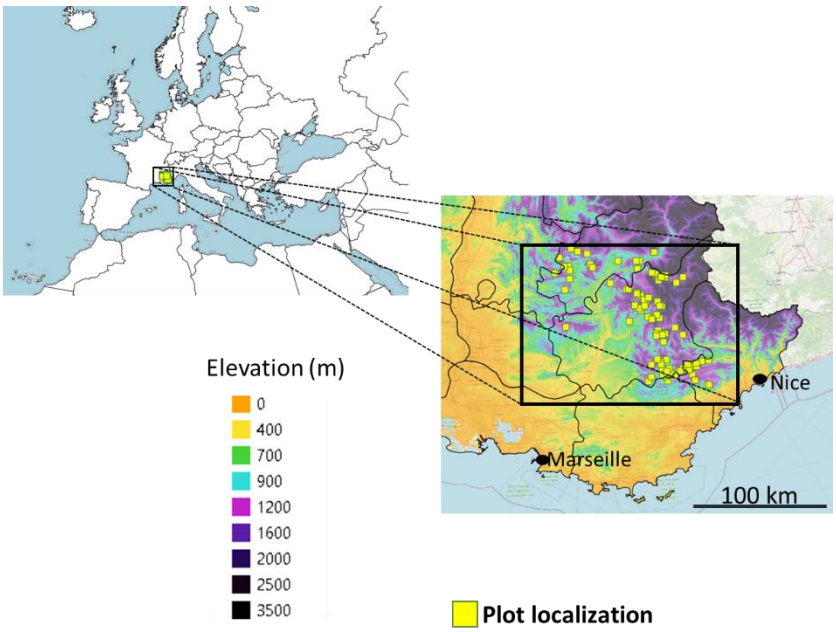

Figure 1. Localization of the 87 plots of Scots pine sampled in southeast France (latitude 43.64–44.58 °N, longitude 5.58–6.93°E).

2.2 Sampling design

Our sample set covered a broad range of soil and climate conditions in which Scots pine was present in the study area (elevation from 600 m to 1700 m; Figure 1). The average annual temperature (1981-2010 period) ranged from 4.8 °C to 12 °C (mean 8.9 °C). Average annual rainfall ranged from 680 mm to 1200 mm (mean 980 mm). Soil type, texture, and bedrock also varied widely, with a pH ranging from 4.5 to 9, and soil depth from 20 cm to 80 cm. Soils were mostly calcareous; but 36% of the plots had acidic soils. No evidence of hydromorphy was observed during our soil measurements.

Based on a bioclimatic model defining the water balance in the French Mediterranean region (Vennetier *et al*., 2008) and earlier studies conducted on the growth and dieback of

Scots pine (Thabeet, 2008; Thabeet *et al*., 2009), three stratification criteria were used to select the plots:

- Elevation: We used two classes, below and above 1200 m ; this elevation corresponding to the boundary between the mountain- and meso-Mediterranean climates (Le Houerou, 2005) and to a marked discontinuity in dieback rates recorded between 2003 and 2006 (Thabeet, 2008).
- Aspect and slope: These were combined in the radiation climate index (IKR) defined by Becker (1984). IKR is computed as the ratio between the solar energy received annually in a given square meter and a reference horizontal square meter at the same place. We used three classes: cold slopes (IKR < 0.95), horizontal areas or neutral slopes (0.95 ≤ IKR < 1.05), and hot slopes (IKR ≥ 1.05).
- Topographic position: The topographic position index TPI_100 (see Appendix A) was computed following Weiss (2001) using a radius of 100 m around the center of the plot. The data came from a digital elevation model (DEM) developed by the French National Institute of Geographic and Forest Information available at a resolution of 25 m (© BDALTI IGN), and was processed using the ©QGis 3.16 software. We chose three classes with contrasting topographical situations: at the bottom of the slope or valley floor (TPI_100 ≤ −0.8, indicating favorable conditions in terms of water balance), mid-slope (−0.8 < TPI_100 < 0.8), and at the top of the slope or on the ridge corresponding to unfavorable conditions (TPI_100 ≥ 0.8).

For each of the 18 combinations obtained (two elevation × three IKR × three TPI_100 classes), five plots were sampled, giving a planned total number of 90 plots. These plots were randomly selected on a systematic 50 x 50 m grid in stands where Scots pine occupied at least 75% of the canopy cover according to the French national forest inventory (© BDFORET v2 IGN). To be finally selected, the plots then had to meet the following criteria: (i) no signs of logging in the last 10 years; (ii) stand height above 3 m or mean

diameter at breast height (DBH) greater than 10 cm to avoid very young stands; (iii) location in a forested area and easily accessible; and (iv) at least 20 pine trees in the dominant or co-dominant overstorey available in homogeneous site conditions around the center of the plot. Sampled plot area ranged from 235 m^2 to 2375 m^2 (mean 522 m^2). 87 plots met all the above criteria.

2.3 Biotic data: health status, dendrometry, and distribution of parasite-prone pine

On each plot, the health status of 20 dominant or co-dominant Scots pine trees was recorded during the 2017 growing season, representing an overall of 1740 trees. We followed the health status monitoring protocol used by the French forest health department (protocol DEPERIS; Goudet, Saintonge, and Nageleisen 2018), which is based on the European protocol used in the ICP-Forests network (Eichhorn *et al*. 2020). A single operator carried out all surveys to limit the estimation bias linked to the measurement protocol.

For each tree, DBH was measured and the functional crown (i.e., free of competition from neighboring trees) was delimited. We used binoculars to estimate on the functional crown and in two opposite directions, the:

- percentage of foliar deficit (FolDef; in %) relative to a healthy reference tree (Figure 2), estimated visually in 5% classes, and that integrates microphylly (needle length < 50% of the regional mean) and the proportion of dead branches;
- number of processionary moth nests per tree (NbnestTp);
- mistletoe abundance as a percentage of the functional crown occupancy (CrownVa; in 5% classes).

Figure 2. Reference photos used in the French and European protocols for estimating crown foliar deficit of Scots pine trees with corresponding defoliation rate in percentage of a fully leafed crown. Source: Müller and Stierlin (1990)

From a subsample of 28 plots representative of all the combinations of stratification classes, two cores per tree were sampled using a Pressler increment borer from the 15 trees closest to the center of the plot and whose health status was recorded (402 trees, i.e., 804 cores were analyzed). After drying and sanding, ring widths were measured to the nearest 0.01 mm on scanned images using Windendro software (WinDENDRO™ 2014, © Regent Instruments Canada Inc.). Each series was visually cross-dated based on the pointer years characterized by particular ring-width, early/latewood ratio or wood anatomy. From the measured ring widths, we computed the basal area increment, which was averaged for five specific periods: during the severe multi-annual drought of 2003–2007 (GSd), before (1997–2002, GSb), and after this event (2008–2016, GSa). The period 2003–2007 was identified locally to have caused a strong reduction in growth and high mortality of Scots pine (Thabeet *et al*., 2009; Vennetier *et al*., 2013). The average basal area increment was then computed considering all years (Gs) and over the last 20 years (1997–2016; Gs20). Finally, considering the non-linearity in the growth trend over this period (see Appendix B), and as tree dieback may be related to a low growth resilience to drought (DeSoto *et a*l., 2020; Trugman *et al*., 2018), we computed the resistance, recovery and resilience indices based on Lloret *et al.* (2011). Resistance (RS) is quantified by the ratio

GSd/GSb, representing the capacity of the trees to buffer stress and maintain growth during drought. Recovery (RC) is the growth reaction following drought and is defined as the ratio GSa/GSd. Resilience (RE) represents the capacity of trees to recover and regain the growth level of the pre-drought period (ratio GSa/GSb). The absence of subsampling bias was checked to ensure that these 28 plots were representative of all 87 plots (Appendix C).

Stand basal area (m^2/ha) was measured using a chain relascope. Finally, because the presence and abundance of mistletoe and processionary moth could be linked to the abundance of tree species sensitive to these pests around the point of measurement (Robinet *et al*., 2014a), we calculated the area occupied around each plot by the pine species locally hosting mistletoe (Scots pine, *Pinus nigra subsp. nigra* Arn. and *Pinus nigra subsp. laricio* (Poiret) Maire) or the pine processionary moth (the same species plus *Pinus halepensis* Mill.). For these two Pine Presence indices (PPI), we tested different radii: 0.2, 0.5, 1, 2, 4, 6, 8, 16, 32 and 64 km, and selected the ones that best explain foliar deficit in the statistical models (see section 2.6).

2.4 Climate data and indices

Mean monthly climatic conditions were characterized for each plot with the AURELHY model for precipitation (P) and minimum and maximum temperatures (Bénichou and Lebreton, 1987). AURELHY provides the 30-year mean values for 1981–2010 at a 1 km resolution, integrating the effects of elevation and topography as far as possible. This model is based on data from 3400 weather stations for rainfall, and 1500 stations for temperature; however, it does not provide extreme values, such as the lowest temperature recorded each year during the 1981-2010 period, an important variable explaining the distribution of the pine processionary moth (see below). This variable has thus been determined with the SAFRAN model, despite its lower spatial resolution (8 km; Quintana-Seguí *et al*., 2008). Mean monthly solar radiation from 1971 to 2000 was estimated with the DIGITALIS model at a 50 m resolution using data from 88 weather stations, taking into account elevation,

263 latitude and topography (Piedallu and Gégout, 2007). Monthly potential evapotranspiration
264 (PET) was estimated with Turc's method (Turc, 1955) to determine a monthly climatic water
265 balance (P-PET). These climatic variables were also calculated for the summer season
266 (June–August), the growing season (April–October), and the non-growing season
267 (November–March).

268 In addition to these climatic variables, we calculated climatic indices of potential
269 colonization by mistletoe and processionary moth. The distribution of mistletoe with
270 elevation and latitude is limited by winter cold and is favored by high summer temperatures
271 (Dobbertin *et al*., 2005). Iversen (1944) developed a climatic index for the presence of
272 mistletoe based on these two criteria. This index was subsequently improved by Skre
273 (1979) in Scandinavia and tested successfully by Dobbertin *et al*. (2005) in Switzerland and
274 by Odland (2009) in Norway. We calculated the Skre index (SKRE_I) for each plot (Eq. 1).

275 $$SKRE\_I = 0.575 \times T_7 + 0.101 \times T_1 - 2.77 \quad \text{(Eq. 1)}$$

276 where T_7 is the mean temperature in July and T_1 the mean temperature in January.

277 Processionary moth dispersion and abundance are also dependent on climatic variables, in
278 particular minimum temperature, radiation, and temperatures in the non-growing season
279 (Hoch *et al*., 2009). For each plot, we tested the climatic variables of the models developed
280 by Robinet *et al*. (2007, 2014), i.e., the absolute minimum temperature, radiation, minimum,
281 maximum, and mean temperatures for each month between October and March, and Turc's
282 evapotranspiration over this 6 months period.

283

284 ## *2.5 Soil and topographic data and indices*

285 **Local topoedaphic index**

286 For each plot, a detailed survey of bedrock, soil and local topography was carried out in the
287 field to calculate a topoedaphic index (TEI) developed and validated over the studied area
288 by Vennetier *et al*. (2018, for details see Appendix D). This index appraises the local water

balance on the plot scale and is correlated with forest productivity. Depending on its value, which ranges from +80 to −80, the water balance is considered as highly favorable (>15), favorable (5 to 15), neutral (−5 to +5), unfavorable (−5 to −15), or highly unfavorable (<−15).

Soil characteristics were estimated directly from a hand-dug trial pit at the center of each plot and from several core drillings throughout the plot. The useful water reservoir was quantified using the protocol of Baize and Jabiol (2011), and calculated from the pedotransfer functions developed by Jamagne *et al*. (1977). The nature of the underlying bedrock was surveyed in the field whenever possible, or else using geological maps. The presence of active limestone was estimated in the top 50 cm using 10% hydrochloric acid. The pH was measured at a depth of 20 cm using a ©SoilStik pH meter. The slope and aspect were measured using a clinometer and a compass.

Topographic indices at landscape scale

Three landscape topographic indices were calculated using two DEMs from the French National Institute of Geographic and Forest Information available with a respective precision of 25 m and 75 m (BD_ALTI © IGN). The topographic position index (TPI) was calculated in a 100 m radius for microtopography (TPI_100, already used for the sampling stratification), and a 1500 m radius (TPI_1500) for macrotopography (Weiss, 2001), with DEMs at 25 m and 75 m resolution respectively, each adapted to a working scale. Plots located at the top of the slope show high TPI values while plots located at the bottom of the valley have low TPI. The topographic wetness index (TWI) is an estimate of the water accumulation in a defined area. It was calculated with DEMs at 75 m. TWI is defined as the ratio of the area upslope (i.e., from where water would flow) from a given point on the landscape to the local slope at that point (Galiano et al., 2010; Petroselli et al., 2013). A high TWI corresponds to favorable situations where water inputs are higher than the losses. These three indices

illustrate the part of the water balance linked to water flows in the landscape, on a larger scale than the plot (i.e., than the TEI).

2.6 Statistical approach

We built two indices quantifying the intensity of colonization by mistletoe and pine processionary moth, and developed three dieback models that related tree and stand health status with all the biotic and abiotic variables mentioned above (Table 1).

Target variables

To quantify the intensity of colonization by biotic factors, we focused on the percentage of crown colonized by mistletoe (CrownVa), and the number of nests of processionary moth per tree (NbnestTp).

For the first dieback model, the percentage of foliar deficit (FolDef) was analyzed on tree scale, while the second model used the percentage of stems with at least 50% of leaf loss (Xstem50) estimated on stand scale. Xstem50 was used instead of the mean foliar deficit as both variables are closely correlated ($r = 0.95$, $p < 0.001$), and Xstem50 is often used operationally by forest managers. Indeed, tree dieback is conventionally defined by a foliar deficit greater than or equal to 50% (DGAL 2018; Linares et Camarero 2012; Sergent 2011). The third model was developed to predict the probability that a stand experiences a dieback, i.e., that its Xstem50 value is greater than 30%. This risk model was designed for direct use in the field by forest managers. Different threshold values of Xstem50 (20, 25 or 30%) are cited in the literature to define dieback in a stand (Brunier *et al.*, 2020; DGAL, 2018; Linares and Camarero, 2012), but preliminary analyses enabled us to retain the 30% threshold (Appendix E).

	Model name	**Target variable *Y***	**Type of variable**	**Statistical approach**
Biotic potential colonization	***Viscum album***	**CrownVa** *mean of crown percentage*	Continuous	PLS

indices		*colonized by mistletoe in the plot*		
	Thaumetopoea pityocampa	**NbnestTp** *Mean number of nests per tree in the plot*	Continuous	PLS
Dieback model	**Tree dieback**	**FolDef** *Tree foliar deficit*	Continuous	Kruskall-Wallis+ PLS
	Stand dieback	**Xstem50** *Percentage of stems in the plot with at least 50% leaf deficit*	Continuous	ANOVA + PLS
	Stand dieback risk	**Xstem50≥30%** *Presence of at least 30% of stems with at least 50% leaf deficit*	Binary	LOG PLS

Table 1. Main characteristics of the biotic colonization indices and dieback models

Summary statistics and model development

A three-way ANOVA was used to determine the pertinence of the stratification variables used for the sampling design: elevation (≥1200 m, <1200 m), IKR (cold, neutral, hot) and TEI (favorable, neutral, unfavorable) on the dieback variables FolDef and Xstem50. ANOVA validity assumptions were statistically examined, i.e., the normality of residuals with the Shapiro-Wilk test, and the homogeneity of variance with the Levene test. Two-by-two comparisons of means were carried out with the Tukey test, except when the variables did not meet ANOVA validity criteria, in which case the Kruskall-Wallis and Nemenyi tests were used.

The two indices of potential colonization by biotic agents and the three dieback models were developed using partial least squares (PLS) regression (Ter-Braak and Juggins, 1993).

The PLS approach is known to well define complex interacting systems (Fernandes, 2012). This regression method predicts the values taken by the target variables from a series of predictor variables using a multivariate approach. This approach sidesteps two difficulties often met in ecology, namely the collinearity of explanatory variables, and the high number of these variables relative to the number of observations (Cramer III *et al*., 1988; Tenenhaus, 1998). The method has proved to be effective in forestry : i.e., to study forest productivity (Bikindou et al., 2012; Paulo et al., 2015; Rathgeber et al., 2005), stand health (Tenenhaus, 1998), and flora composition based on a bioclimatic model (Vennetier et al. 2008). We chose the PLS approach because the number of variables used to build the models was large (99 in total, see Appendix A) and exceeded the number of plots. Also, some climatic and topographic variables based on digital elevation models are highly correlated. For instance, The AURELHY and DIGITALIS models use topography information to derive high-resolution climatic maps (Bénichou and Lebreton, 1987; Piedallu and Gégout, 2007). A stepwise method based on the Q^2 coefficient of Stone-Geisser was used to select the number of components in the PLS regression (Bertrand, F., Maumy-Bertrand, M., 2018; Bastien, P., Vinzi, V.E., Tenenhaus, M., 2005). Only the variables whose partial correlation coefficient was significantly different from zero ($p < 0.05$) after bootstrapping were then retained. To model the probability of the presence or absence of dieback in a plot, we used a PLS binary logistic regression approach (LOG PLS); the logistic regression being regularly used to predict tree mortality risk (e.g., Cailleret *et al*., 2016; Hülsmann *et al*., 2018; Monserud, 1976). The LOG PLS combines a PLS regression model with the binary prediction model of logistic regression. The PLS regressions were run with the plsRglm package (Partial Least Squares Regression for Generalized Linear Models; Bastien *et al*., 2005; Bertrand and Maumy-Bertrand, 2018) from the R 4.0.5 open-source software (RStudio Team, 2021).

Finally, we partitioned the variance of the stand dieback models to assess the relative weights of the biotic, climatic, and topoedaphic factors. Venn diagrams were drawn with the

383 eulerr R package (Larsson, 2021) to evaluate the specific and combined weights of these
384 three groups of variables in the explained variance of Xstem50 and of biotic potential
385 colonization indices. In such diagrams, the area of the ellipse plotted for each group is
386 proportional to the sum of its individual coefficient of determination and its joint contribution
387 with one or several other groups. The joint contributions are represented by the area of the
388 intersections of the individual ellipses.
389

390 ## 3. Results

391 The stands studied were relatively young, 88 years on average, with a quite broad range of
392 tree age and diameter between and within plots (Table 2 and Appendix F). This variability is
393 related to the gradual recolonization of abandoned farmlands by Scots pine over the last
394 century (Médail, 2001). Their health status is poor; the foliar deficit (FolDef) and percentage
395 of stems with more than 50 % of foliar deficit (Xstem50) respectively averaged 48% and
396 31% (Table 2). No plot showed less than 25% of foliar deficit, and 51% of the plots were
397 considered as declining as XStem50 was higher than 30%. A broad variability in the
398 presence and abundance of biotic agents was observed between plots: mean crown
399 infestation by mistletoe in the crown ranged from 0 to 29%, and the mean number of
400 caterpillar nests per tree ranged from 0 to 6 (for details see Appendix G).
401

Variable	Mean	Standard deviation	Min	Max
Age (years)	88	30	48	181
Diameter at breast height (cm)	26	4.6	17	40
Stand basal area (m^2/ha)	23.1	8.8	8	48
FolDef (%)	48.3	11.7	25.8	84.5
Xstem50 (%)	31	24.9	0	90
NbnestTp	0.66	1.25	0	6
CrownVa (%)	8.1	7.6	0	29

402 **Table 2.** Main stand characteristics. The target variables are defined in Table 1.

3.1 Influence of elevation, IKR, and topoedaphic index

Below 1200m of elevation, the mean tree foliar deficit (FolDef) and the percentage of stems in the plot with at least 50% of leaf deficit (Xstem50) were significantly higher than above this threshold ($p < 0.05$; Figure 3A and 3D; Appendix H). The effect of IKR was less obvious as there were no significant differences in Xstem50 (Figure 3E), and only the trees growing in the hot situations had higher FolDef ($p<0.01$; Figure 3B). FolDef and Xstem50 were higher in the unfavorable topoedaphic situations than in the neutral and favorable classes, while the difference between these two classes were only significant for FolDef (Figure 3C and 3F). There were no interactive effects of the elevation, IKR and TEI classes on both dieback variables.

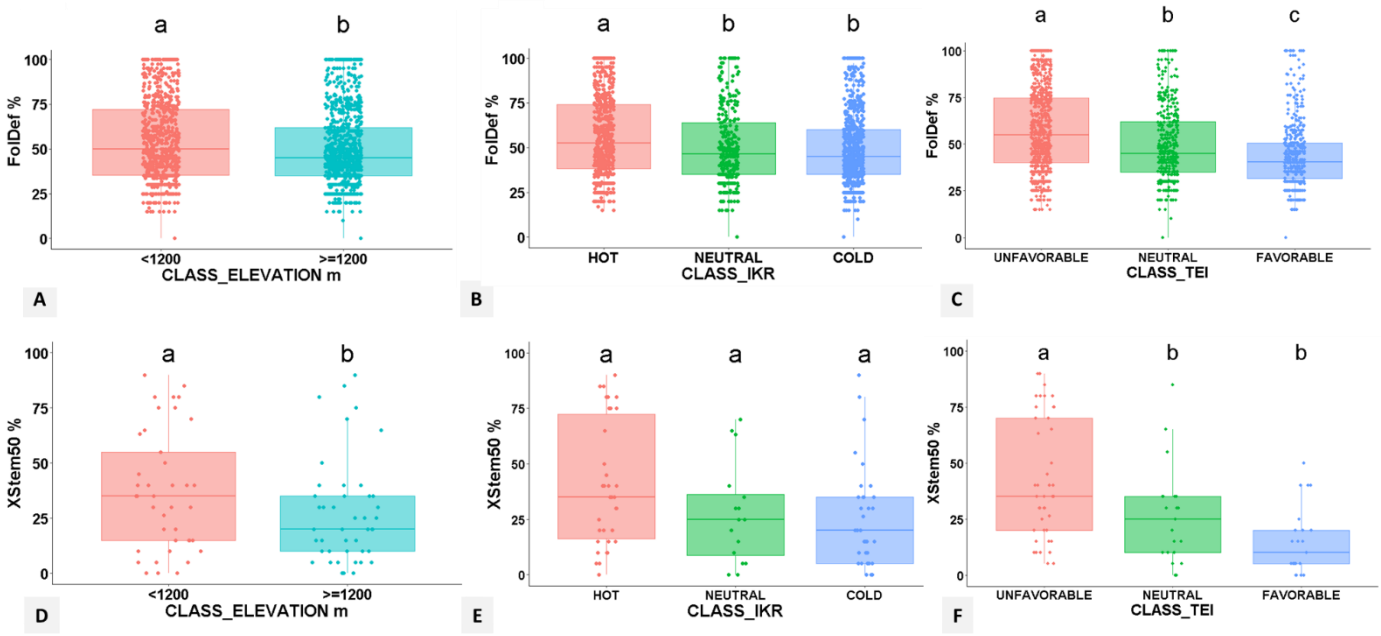

Figure 3. Differences in tree foliar deficit (FolDef, %; *Top*) and in stand XStem50 (%; *Bottom*) between classes of elevation (A and D), IKR (B and E) and topoedaphic index (TEI; C and F). Rectangles delimit two central quartiles separated by the median. Points indicate the value of each tree (A, B, C) or each stand (D, E, F). Groups sharing the same letter did not differ significantly ($p < 0.05$).

3.2 Potential colonization indices for mistletoe and processionary moth

The proportion of the crown colonized by mistletoe (CrownVa) was highly correlated with biotic, climatic, and topoedaphic factors (R^2 = 0.38, p < 0.001; Table 3 and Figure 4). Concerning the biotic factors, it was positively impacted by the cumulative area of pine species sensitive to mistletoe (pine presence index; PPI) in an 8 km radius around the studied plot. Mistletoe was more abundant when water deficit was marked (i.e., low P-PET), and when mean January and July temperatures (Skre index) were high. Likewise, mistletoe was more abundant in situations with unfavorable topography, where temperatures are higher and the water balance lower, such as on convex terrain or at the top of the slope (low TEI and high TPI_100). In the PLS regression, climatic variables had standardized coefficients that are ~2 times higher than those of the other variables with significant effects, highlighting the strong importance of climate on the colonization by mistletoe.

Like mistletoe, the number of processionary moth nests per tree (NbnestTp) was closely correlated with biotic, climatic, and topoedaphic variables (R^2 = 0.32, $p \leq 0.001$; Table 3 and Figure 4). The PPI and climatic variables had the highest standardized coefficients in absolute values; PPI being positively associated with the number of nests, but this time in a radius of 6 km. The PET from October to March and the absolute minimum temperature also influenced significantly and positively the number of nests. The warmer the winter months, the more nests were found. Finally, the two topographic factors TEI and TPI (here TPI_1500) were significant, as they were for mistletoe. Caterpillars were more abundant in situations with unfavorable topography and water balance (low TEI) such as on convex terrain or at the top of the slope (high TPI_1500).

	Number of components of the PLS	**Q^2**	**RSS**	**$\sum R^2Y$**
Biotic index for mistletoe Potential colonization index of *V. album* **CIVA**	**1**	0.34	3067	0.38
Biotic index for processionary moth Potential colonization index of *T. pityocampa* **CITP**	**1**	0.25	91	0.32

Tree dieback model *FolDef (%)*	**1**	0.32	97613	0.33
	2	0.34	90580	0.38
Stand dieback model *Xstem50 (%)*	**1**	0.62	20228	0.65
		CHI^2	**Misclassified***	**AUC**
Stand dieback risk model *Xstem50 ≥ 30%*	**1**	67	21.6%*	0.88

436 **Table 3**. Summary statistics for the different Partial Least Square (PLS) regression models.
437 Q^2 the coefficient of Stone-Geisser, RSS the Residual Sum of Squares, $\sum R^2Y$ the
438 coefficient of determination, and AUC the Area Under the receiver operating characteristics
439 Curve.* The misclassification rate was calculated by cross-validation
440

Biotic indexes

Potential Colonization Index of *V.album* CIVA

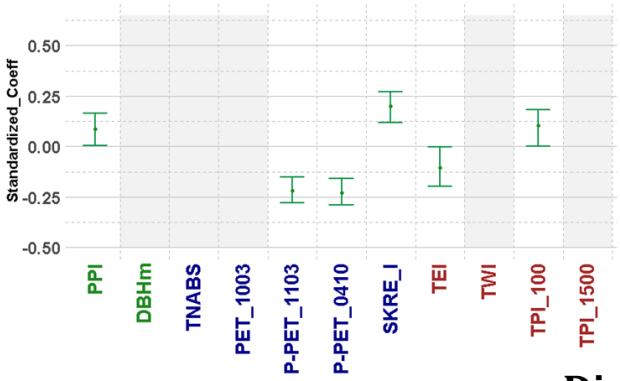

Potential Colonization Index of *T.pityocampa* CITP

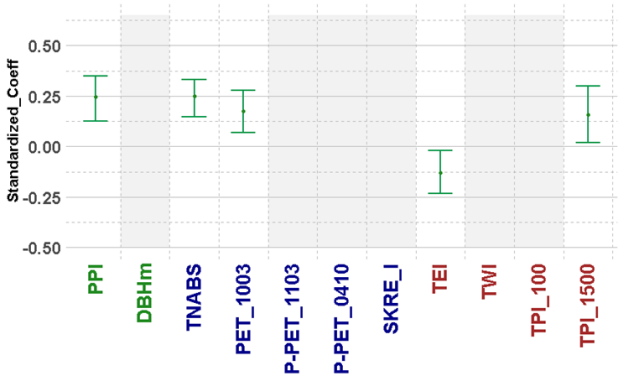

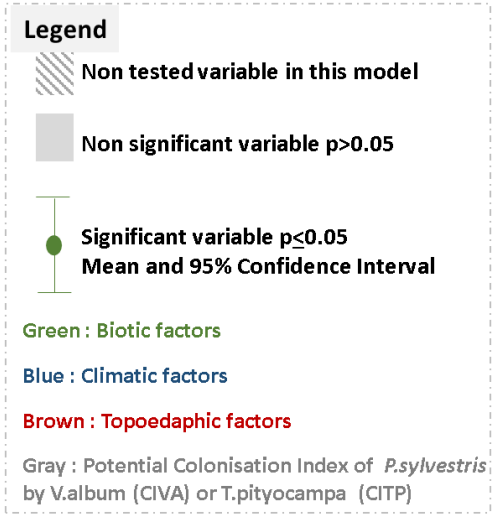

Dieback models

Tree dieback FolDef %

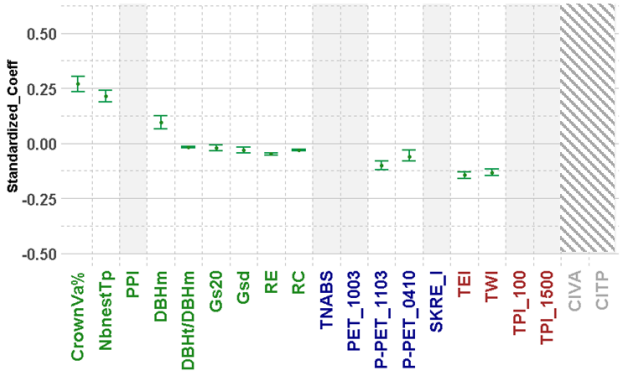

Stand dieback XStem50 %

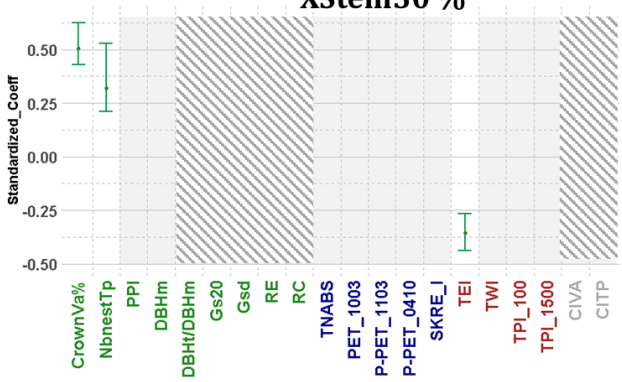

Risk model XStem50≥30%

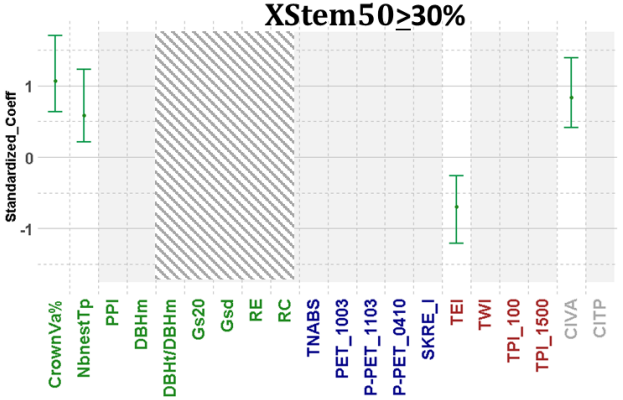

441

Figure 4. Standardized partial correlation coefficients of the significant variables selected in the Partial Least Squares regression models developed to predict the potential colonization of the biotic factors, and to predict tree and stand dieback. *CrownVa%* is the percentage of pine crowns colonized by mistletoe (% per tree or per plot according to the model); *NbnestTp* is the number of processionary moth nests (per tree or per plot according to the model); *PPI* is the Pine Presence Index expressed in area occupied by pine species sensitive to mistletoe or to pine processionary moth (ha; calculated in a radius of 8 km and 6 km, respectively); *DBHm* is the mean stand DBH (cm); *DBHt/DBHm* is the ratio between tree DBH and the mean stand DBH; *Gs20* is the mean BAI over the last 20 years (1997–2016 ; mm²/year); *Gsd* is the mean BAI during the major climatic stress (2003-2007; mm²/year); *RE* is the resilience, defined as the ratio between mean BAI after drought (2008-2016; Gsa) and before drought (1997-2002; Gsb); *RC* is the recovery, defined as the ratio between mean BAI after drought (2008-2016; Gsa) and during drought (2003-2007; Gsd); *P-PET_1103* and *P-PET_0410* are the difference between precipitation and potential evapotranspiration calculated from November to March, and from April to October, respectively; *SKRE_I* is the Skre index (see eq. 1). *PET_1003* is the potential evapotranspiration October to March; *TNABS* is the absolute minimum temperature (°C); *TEI* is the field-based topoedaphic index; *TWI* is the topographic wetness index; *TPI_100* and *TPI_1500* are the topographic position indices calculated using 100m and 1500m radii, respectively. Finally, *CIVA* and *CITP* are the potential colonization indices calculated for *V. album* and *T. pityocampa*, respectively. All climatic variables are calculated for the 1981-2010 period.

3.3 Dieback models

Tree model

The model explaining the foliar deficit of the 402 cored trees had a coefficient of determination of 0.38 with 12 significant variables (Table 3 and Figure 4). The two most influential variables were the percentage of the crown colonized by mistletoe (CrownVa) and the number of caterpillar nests (NbnestTp) per tree, which were positively correlated with foliar deficit. Then, in decreasing order of importance, came the topographic wetness index (TWI) and the topoedaphic index (TEI), for which the foliar deficit was negatively correlated, followed by the summer and winter climatic water balance (P-ETP), which positively influence tree health status (negative correlation with foliar

deficit). Trees that grow the best, i.e., with higher mean BAI over the last 20 years (Gs20), and that best experienced the 2003-2007 drought (high Gsd, resilience RE and recovery RC values) showed the lowest foliar deficit. Finally, stand mean DBH was positively correlated with the foliar deficit; but in these stands, the suppressed trees (with a low DBHt/DBHm ratio) tend to be more defoliated.

Stand model

At stand scale, the model predicting Xstem50 had the highest coefficient of correlation (R^2 = 0.65; Table 3). It involved three variables, CrownVa, TEI and NbnestTp, in order of decreasing importance. A high mean abundance of mistletoe and caterpillar nests increased the percentage of stems with at least 50% of foliar deficit; and both biotic factors contributed to 42.3% of the explained variance in Xstem50 (Figure 5A). The stand dieback level was lower in favorable topoedaphic conditions (high TEI), whose contribution on the variance in Xstem50 is limited when analyzed alone (5.6%), but much higher when considering its joint contribution with the biotic variables (16.6%; Figure 5 A). This model does not emphasize the direct effect of climatic variables on Xstem50, but the climate is involved indirectly via its contribution in the PLS regressions quantifying the potential colonization of mistletoe (it explained 31.5% of the variance; Figure 5B) and of the processionary moth (19.6% of the variance; Figure 5C).

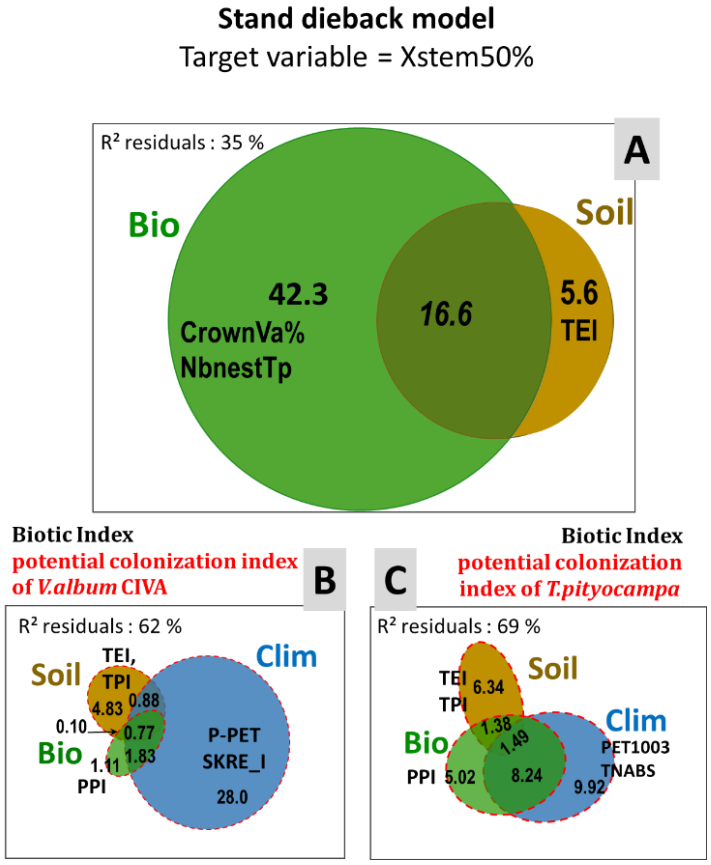

Figure 5. Venn diagrams for the stand dieback model and the two biotic colonization indices: mistletoe and processionary moth. The independent and joint contribution of each type of variable (defined in Figure 4) is expressed as respectively the area of circles and of their intersections, which are proportional to their contribution to the explained variance of the model.

The interaction between the climatic factors and biotic factors explains part of the variability in dieback observed among stands (Figure 6). In the situations where mistletoe was present in the field, Xstem50 increased with the mistletoe potential colonization index (CIVA index), and indicator of favorable environmental conditions. In contrast, when mistletoe was absent, the percentage of stems with dieback did not increase with these favorable conditions (Figure 6). Stand health status was thus degraded when the presence of mistletoe in the field is combined with warm and dry climate and topoedaphic conditions. In contrast to mistletoe, the number of processionary moth nests did not act as interactive factor with climate, but as additive effect (Figure 6). The presence of nests increased defoliation in the plots significantly ($p < 0.05$), on average by 10 %, irrespective of whether mistletoe was present in the field.

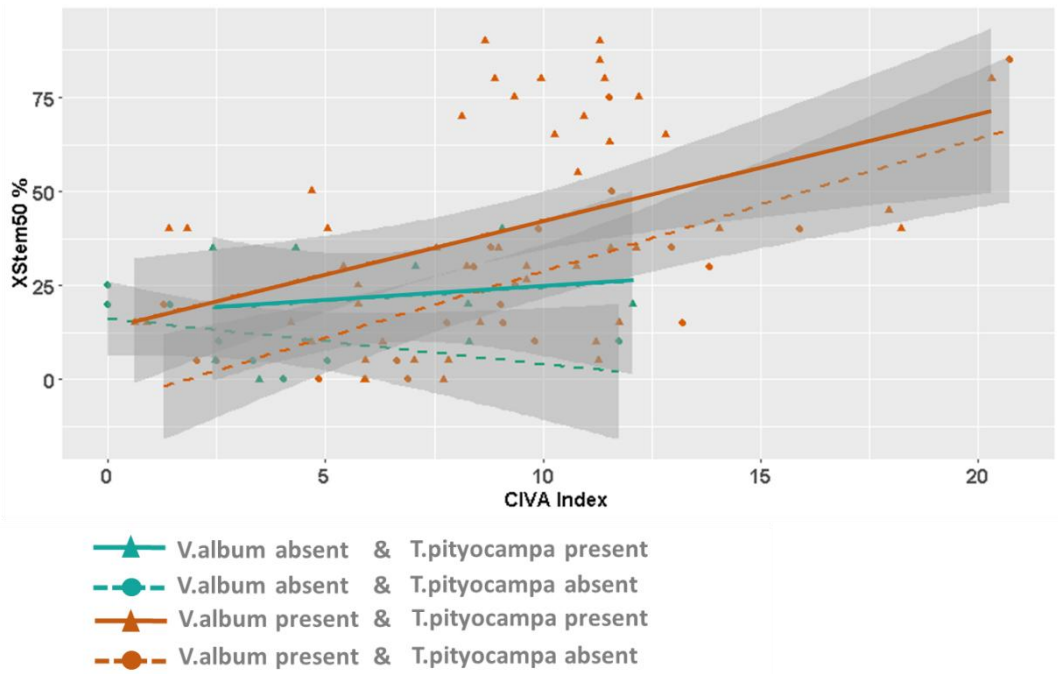

Figure 6: Xstem50 as a function of the potential colonization index for mistletoe (CIVA index) and according to the actual presence or absence of mistletoe and processionary moth on the plot.

Risk model

The dieback risk model developed here performed well: its cross-validation misclassification rate was 21.6%, and its AUC was 0.88 indicating an excellent predictive quality (Hosmer *et al*., 2013). It tends to lightly overestimate dieback proportion in medium risk classes, i.e., when the dieback risk predicted by the model is between 20 and 80%, the proportion of stand with observed dieback is lower than expected (Figure 7).

Four variables were significant in this model; two of these were linked to mistletoe (Figure 4). The first was its potential colonization (CIVA) index, which integrates biotic (PPI), climatic, and soil factors (Figure 6B). The second was its actual presence in the field (CrownVa). Introduction of these two variables in the risk model takes account of the interaction between the presence of mistletoe and the environmental conditions prone to its development (underlying factors in the CIVA index). The other two variables were also included in the stand model, namely the topoedaphic index and the average number of processionary caterpillar nests per tree. Although only marginally significant (p = 0.06) and consequently not considered in the

best model (Figure 4), the processionary moth potential colonization index (CITP) confirmed the indirect influence of climatic variables on dieback risk.

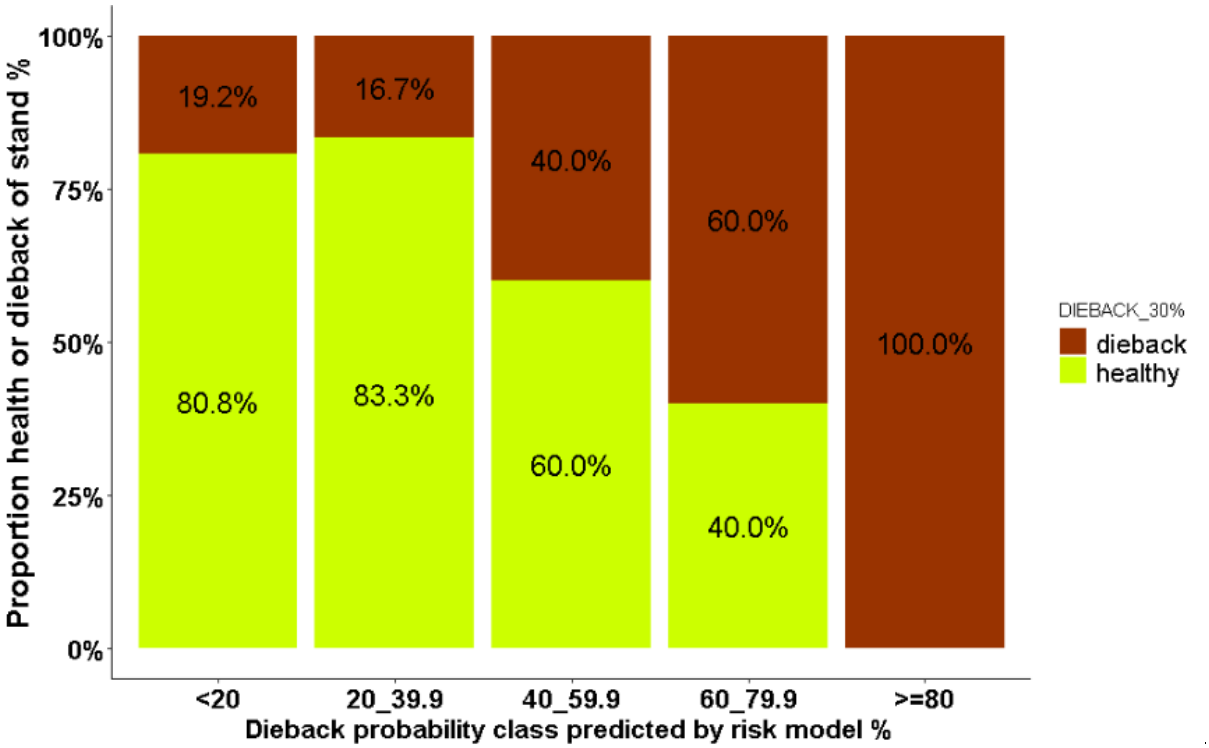

Figure 7. Distribution of healthy stands (Xstem50<30%) or stands with dieback (Xstem50≥30%) by the dieback probability class as predicted by the risk model. These 20% classes were set to include at least five plots each. Significant differences in the proportion of plots with observed dieback were observed between risk classes predicted by the model (chi-square = 40.17, df = 4, $p < 0.001$).

4. Discussion

Tree dieback is a complex process that requires a multifactorial and multiscale approach (Franklin *et al*. 1987; Manion 1991; Allen *et al*. 2015). This study, based on multivariate statistical models and conducted on Scots pine, confirms the importance of incorporating a range of biotic factors (tree and stand characteristics, and abundance of mistletoe and processionary moth), topographic and soil factors representing the local- and landscape-scale water balance, and climatic factors, which are important both directly and through their interactions with the other factors.

4.1 Biotic factors

Mistletoe and the pine processionary moth play essential roles in the Scots pine dieback process. When considering their interaction with the topoedaphic variables, these biotic factors explain 64.5% of the variance in the percentage of stems with 50% of leaf deficit (stand model predicting Xstem50 ; Figure 5).

The impact of mistletoe on the health and growth of Scots pine is well documented. Mistletoe does not regulate its transpiration even under drought, and consequently reduces the water available to the host tree, worsening its physiological stress. It also uses a significant proportion of the nutrients from the tree sap, which it stores in its own structure (Mutlu *et al*., 2016). Consequently, infested trees close their stomata earlier and longer (Zweifel *et al*., 2012) and produce smaller leaves (Rigling *et al*., 2010) thereby limiting their carbon absorption capacity and growth potential (Meinzer *et al*., 2004). Stand-scale productivity losses have been estimated at between 29% in Germany (Kollas *et al*. 2018) and 64% in Spain for high levels of infestation (Camarero *et al*., 2018), with lower resistance and resilience to severe drought. Infestation by mistletoe is on average more marked in the upper part of the crown due to the parasite's heliophilous nature (Briggs, 2021; Mellado and Zamora, 2014) and the behavior of the birds that spread it. This explains why it was mostly present in our study area in sunny locations such as on convex terrain (high TPI; Figures 4 and 5), and in open stands.

The presence of mistletoe is also linked to climate (Jeffree and Jeffree, 1996), especially to temperatures in the coldest and hottest months, as shown by its significant correlation with the Skre index (Figure 4). Although temperature is the variable that best explains the presence of mistletoe, the population density of fruit-eating birds, and more specifically of its main dispersion agent the thrush genus *Turdus*, also explains the spatial distribution of mistletoe at landscape scale (Ramsauer *et al*., 2021). The most significant radius (8 km) used to calculate the area of pines sensitive to mistletoe around our plots is in line with the literature, e.g., with the minimum radius of 3.5 km estimated in Catalonia by Ramsauer *et al*. (2021). The propagation of mistletoe from a point source is fast, accelerates over time with the progressive increase in population density in neighboring areas, but is still modulated by vegetation distribution in the landscape and

562 especially by the availability of host species (from 0.04 km/year to 0.35 km/year ; Hawksworth and
563 Scharpf 1986, Shaw and Lee 2020).

564 The processionary moth is a forest pest that can cause severe damage to leaves, especially in
565 newly infested areas (Battisti *et al*., 2005; Stastny *et al*., 2006). Its distribution in our study area
566 was closely linked to climate, to the area covered by pine stands on the landscape, and to soil and
567 topography factors. The potential evapotranspiration from October to March and minimum
568 absolute temperature were the two dominant climatic variables in the colonization model, in line
569 with the model of Robinet *et al*. (2007) calibrated in central France. Low minimum temperature
570 limits the expansion of the processionary moth toward higher elevations and latitudes (Hoch *et al*.,
571 2009; Hódar *et al*., 2003) as it needs heat in winter and large amounts of sunlight to feed and
572 survive (Battisti *et al*., 2005). It is accordingly found on sunny exposition (e.g., at the top of the
573 slopes, south-facing aspect; Figures 4 and 5) and in open forests where tree canopies are well
574 exposed. The optimal radius to compute its pine hosts density (6 km), is consistent with the study
575 by Robinet *et al*. (2014b), stating that females can fly 6 km on average, and up to 10 km.

576 The density of both mistletoe and processionary moth populations seem thus reduced when the
577 stands sensitive to these parasites are young, have low stand density, and are scattered over the
578 landscape (low PPI; see also Shaw and Lee 2020). Because Scots pine naturally and gradually
579 colonized abandoned farmland over the last century (Médail, 2001), its age and spatial distribution
580 is irregular within the landscape. This explains why some plots were not or only slightly affected by
581 these parasites, and thus relatively healthy, despite climatic and site conditions favorable to these
582 pests (Figure 6). Such plots, though few in number, reduced the predictive capacity of the dieback
583 models by partly masking the effects of climatic variables.
584
585 For these two heliophilous parasites, the significant weight of topography and soil is explained by
586 their relationship with the water balance and landscape structure. Stands located at the top of the
587 slopes, on ridges, on convex terrain well-exposed to sunlight, and on shallow or stony soils (often
588 found in such locations due to erosion), (i) usually have a low stem density and canopy cover
589 favoring the infestation of dominant trees with sunny crowns, and (ii) have limited water retention

capacities, weakening trees and increasing their vulnerability to these parasites and so accelerating dieback (Mutlu *et al*., 2016). These stands have especially experienced high defoliation and mortality rates during and following the 2003–2007 drought (Vennetier *et al*., 2007), opening them, and favoring both mistletoe and processionary moth populations.

Independently of the factors cited above, stands with large mean tree DBH had higher foliar deficit (see also Galiano et al. 2010). These large trees generally have larger crowns, which would be preferred by both mistletoe and processionary moth that demand light. They also provide more sites for birds involved in the spread of mistletoe (Kolodziejek J and Kolodziejek A, 2013). Nevertheless, in these stands, shaded trees smaller than the stand average had higher foliar deficits, probably due to the relative intolerance of Scots pine to high levels of shade (Gaudio et al., 2011). This result is supported by the studies from Taccoen *et al*. (2021) who reported an excess of mortality in shaded Scots pine in South-East France linked to the climate and its change, and from Galiano *et al*. (2010) in the Spanish Pyrenees.

Finally, trees with the lowest foliar deficit were also those with the higher mean growth over the last 20 years, and with the higher recovery and resilience after the 2003-2007 drought. The causal link between growth and crown health (i.e., defoliated trees show low growth rates and recovery after drought, or trees with low growth and recovery rates are more sensitive to further drought and prone to dieback) is unclear because the information on the temporal change in foliar deficit is missing. However, the negative relationships between foliar deficit and mean growth rates and resilience to drought were consistent with previous physiological and dendroecological studies (e.g., DeSoto *et al*., 2020; Dobbertin, 2005; Guada *et al*., 2016; Poyatos *et al*., 2013). Interestingly, growth resistance to drought does not seem related to Scots pine dieback, just as it does not seem related to the mortality of gymnosperms (DeSoto *et al*., 2020).

4.2 Climatic factors

Climatic variables alone only partly explained tree dieback in the PLS regression models. The more unfavorable the climatic water balance (P-PET) during the growing and non-growing seasons, the

higher the foliar deficit, reflecting the well-known sensitivity to drought of Scots pine (e.g., Camarero et al., 2015; Galiano et al., 2010; Matías et al., 2017; Rigling et al., 2013). These climatic variables were calculated for the period 1981–2010. This period was warmer than the previous decades (Cramer et al., 2018), thus favorable towards the dissemination of mistletoe with more effects on the health of stands.

This period also corresponded to the first reports of massive dieback in southeast France, partly linked to the presence of biotic agents and drought (Lieutier et al., 1988; Sardin, 1997). As previously shown, the strong interactions of climate with biotic and topoedaphic factors (Figure 6), added to the irregular spatial distribution of these biotic agents on the regional scale, probably limited the ability of the models to isolate the impact of some climatic variables.

4.3 Soil and topography factors

Our analysis highlights a strong effect of topographic and edaphic conditions on foliar deficit, which are important in offsetting or worsening climatic water balance. Scots pine presents high foliar deficits on shallow soils (i.e., low TEI) with low water holding capacity (Galiano *et al*. 2010) but also low growth rate (Bigler *et al*. 2006).

The topoedaphic index (TEI) had a significant effect in all the dieback models developed, confirming its relevance to assess at least roughly the water balance at local scale, independently of the vegetation and climate. A more accurate quantification of this water balance could be obtained from fine soil measurements and from the evaluation of the water demand at stand scale (e.g., with the leaf area index; see Granier *et al*., 2000), but would require additional work beyond our possibilities. Operationally, the TEI offers the advantage of being of use in varied topographic conditions, notably in conditions where slope or hillside effects are very marked, such as in our study area.

However, this index still needs calibration at regional scale and to be evaluated in other contexts, and is not sufficient to estimate water fluxes and pools at landscape level. Topographic indices calculated from DEMs on a scale of 100 m (microtopography) or 1500 m (macrotopography) must also be integrated, as revealed by our tree dieback model and several previous studies (Petroselli et al., 2013; Raduła et al., 2018; Kopecký et al., 2021).

4.4 Comparison of dieback models

The model developed at tree level had quite low performance (R^2 = 0.38), which may partly due to the difficulties when estimating tree leaf deficit despite a careful application of the protocols. The presence of understorey may limit the view of the functional crown in several directions and the microphylly, which is very frequent in our study area, is not easy to estimate with binoculars. However, this was mainly caused by the high variability in foliar deficit within stands (see Table 3), which was only partly captured by the variables measured at tree scale (age, diameter, and annual radial growth). The integration of an individual-based competition index (e.g. Heygi index 1974) could have improved the predictive ability of the tree model (e.g. Galiano et al., 2010).

In the geologically complex environments we studied, the vertical and horizontal heterogeneity in soil properties (e.g., texture, percentage of coarse elements) and in bedrock fracture levels was very high, sometimes only a few meters away, and could not be evaluated with a single soil pit. This intra-plot variability in foliar deficit can also be linked to different microclimatic conditions between trees depending on their neighborhood and on the micro-topography. Some trees have also undergone other climatic damages, such as snow breaks, often observed in these environments (Vennetier *et al*. 2007). They may have different genetic potential, for example causing differences in water use efficiency, even though this effect of genetic differentiation may be negligible (Santini et al., 2018).

At stand scale, the models predicting the percentage of declining tree (i.e., with a foliar deficit higher than 50%), and the probability of having more than 30% of declining trees model offered a higher prediction quality (R^2 = 0.65 and AUC = 0.88, respectively). The risk model reliably predicted dieback in successive 20% classes (Figure 7), making it operational for a direct use in the field; although a slight tendency to overestimate dieback between 20 and 80% was noted. This model seems to offer a valuable support for decision-making in forest management in a context of increasing drought recurrence and intensity.

This modeling approach was designed to be continuously improved, generalized to all tree species and other pedoclimatic contexts, and enhanced by the improved quality and availability of foliar deficit data, for example at European scale (Ferretti, 2021). Another option was to make the risk

model available as an application to allow simple diagnostics in the field and make use of data collected by users, so increasing the size and diversity of the database used for calibration and validation. This would make the model more general, i.e., of use in regions where other abiotic or biotic factors are involved in the dieback process (e.g., presence of other pathogens, high competition intensity, hydromorphy; see Oliva *et al.*, 2016 or Taccoen *et al.*, 2021).

5. Conclusion

This work emphasizes the importance of taking into account the respective and interactive effects of multiple abiotic and biotic environmental factors to model tree foliar deficit and dieback. The abiotic factors cannot be reduced to the climatic conditions alone and must also include soil variables observed in the field and the local and landscape topography, which contribute to the local water balance. Finally, the abundance of biotic factors, here processionary moth and mistletoe, is of key importance to accurately predict foliar deficit and dieback of Scots pine. Considering that their potential colonization on the host pine tree is also dependent of biotic, climatic, soil and topographic factors, this study highlights the interdependencies between biotic agents and abiotic factors.

6. Acknowledgments

We warmly thank the Provence-Alpes-Côtes-d'Azur Region and the RMT Aforce for funding this project, the French 'Département Santé des Forêts' for scientific support, and the 'Centre Régional de la Propriété Forestière' of the Provence-Alpes-Côte-d'Azur Region who coordinated the research project behind this work. Authors are indebted to Poncet M., Perry H., Marty P. and Jourdan A. who contributed to field work and data processing.

7. References

Adams, H.D., Germino, M.J., Breshears, D.D., Barron-Gafford, G.A., Guardiola-Claramonte, M., Zou, C.B., Huxman, T.E., 2013. Nonstructural leaf carbohydrate dynamics of Pinus edulis during drought-induced tree mortality reveal role for carbon metabolism in mortality mechanism. New Phytol. 197, 1142–1151. https://doi.org/10.1111/nph.12102

Allen, C.D., Macalady, A.K., Chenchouni, H., Bachelet, D., McDowell, N., Vennetier, M., Kitzberger, T., Rigling, A., Breshears, D.D., Hogg, E.H. (Ted), Gonzalez, P., Fensham, R., Zhang, Z., Castro, J., Demidova, N., Lim, J.-H., Allard, G., Running, S.W., Semerci, A., Cobb, N., 2010. A global overview of drought and heat-induced tree mortality reveals emerging climate change risks for forests. For. Ecol. Manag., Adaptation of Forests and Forest Management to Changing Climate 259, 660–684. https://doi.org/10.1016/j.foreco.2009.09.001

Anderegg, W.R.L., Kane, J.M., Anderegg, L.D.L., 2013. Consequences of widespread tree mortality triggered by drought and temperature stress. Nat. Clim. Change 3, 30–36. https://doi.org/10.1038/nclimate1635

Baize, D., Jabiol, B., 2011. Guide pour la description des sols, Quae. ed.

Bastien, P., Vinzi, V.E., Tenenhaus, M., 2005. PLS generalised linear regression. Comput. Stat. Data Anal., Partial Least Squares 48, 17–46. https://doi.org/10.1016/j.csda.2004.02.005

Battisti, A., Stastny, M., Netherer, S., Robinet, C., Schopf, A., Roques, A., Larsson, S., 2005. Expansion of Geographic Range in the Pine Processionary Moth Caused by Increased Winter Temperatures. Ecol. Appl. 15, 2084–2096. https://doi.org/10.1890/04-1903

BD ALTI® | Géoservices [WWW Document], n.d. URL https://geoservices.ign.fr/bdalti (accessed 9.6.21).

Becker, M., Bräker, O.U., Kenk, G., Schneider, O., Schweingruber, F.H., 1990. Appearance of crowns and growth of trees in the last few decades in the border regions of Germany, France and Switzerland [WWW Document]. URL https://doi.org/10.4267/2042/26075

Bénichou, P., Lebreton, O., 1987. Prise en compte de la topographie pour la cartographie des champs pluviométriques statistiques. La météorologie 7è série, 23–34.

726 Bertrand, F., Maumy-Bertrand, M., 2018. plsRglm: Partial least squares linear and generalized
727 linear regression for processing incomplete datasets by cross-validation and bootstrap
728 techniques with R. ArXiv181001005 Stat.
729 Bigler, C., Bräker, O.U., Bugmann, H., Dobbertin, M., Rigling, A., 2006. Drought as an Inciting
730 Mortality Factor in Scots Pine Stands of the Valais, Switzerland. Ecosystems 9, 330–343.
731 https://doi.org/10.1007/s10021-005-0126-2
732 Bigler, C., Bugmann, H., 2004. Predicting the Time of Tree Death Using Dendrochronological Data.
733 Ecol. Appl. 14, 902–914. https://doi.org/10.1890/03-5011
734 Bikindou, F.D.A., Gomat, H.Y., Deleporte, P., Bouillet, J.-P., Moukini, R., Mbedi, Y., Ngouaka, E.,
735 Brunet, D., Sita, S., Diazenza, J.-B., Vouidibio, J., Mareschal, L., Ranger, J., Saint-André, L.,
736 2012. Are NIR spectra useful for predicting site indices in sandy soils under Eucalyptus
737 stands in Republic of Congo? For. Ecol. Manag. 266, 126–137.
738 https://doi.org/10.1016/j.foreco.2011.11.012
739 Bréda, N., Huc, R., Granier, A., Dreyer, E., 2006. Temperate forest trees and stands under severe
740 drought: a review of ecophysiological responses, adaptation processes and long-term
741 consequences. Ann. For. Sci. 63, 625–644. https://doi.org/10.1051/forest:2006042
742 Briggs, J., 2021. Mistletoe, Viscum album (Santalaceae), in Britain and Ireland; a discussion and
743 review of current status and trends. Br. Ir. Bot. 3. https://doi.org/10.33928/bib.2021.03.419
744 Brunier, L., Delport, F., Gauquelin, X., 2020. Guide de gestion des crises sanitaires en forêt., CNPF-
745 IDF. ed.
746 Cailleret, M., Bigler, C., Bugmann, H., Camarero, J.J., Cˇufar, K., Davi, H., Mészáros, I., Minunno,
747 F., Peltoniemi, M., Robert, E.M.R., Suarez, M.L., Tognetti, R., Martínez-Vilalta, J., 2016.
748 Towards a common methodology for developing logistic tree mortality models based on ring-
749 width data. Ecol. Appl. 26, 1827–1841. https://doi.org/10.1890/15-1402.1
750 Camarero, J.J., Gazol, A., Sangüesa-Barreda, G., Oliva, J., Vicente-Serrano, S.M., 2015. To die or
751 not to die: early warnings of tree dieback in response to a severe drought. J. Ecol. 103, 44–
752 57. https://doi.org/10.1111/1365-2745.12295
753

754 Camarero, J.J., Tardif, J., Gazol, A., Conciatori, F., 2022. Pine processionary moth outbreaks cause
755 longer growth legacies than drought and are linked to the North Atlantic Oscillation. Science
756 of The Total Environment 819, 153041. https://doi.org/10.1016/j.scitotenv.2022.153041
757 Carnicer, J., Coll, M., Ninyerola, M., Pons, X., Sánchez, G., Peñuelas, J., 2011. Widespread crown
758 condition decline, food web disruption, and amplified tree mortality with increased climate
759 change-type drought. Proc. Natl. Acad. Sci. 108, 1474–1478.
760 https://doi.org/10.1073/pnas.1010070108
761 Choat, B., Jansen, S., Brodribb, T.J., Cochard, H., Delzon, S., Bhaskar, R., Bucci, S.J., Feild, T.S.,
762 Gleason, S.M., Hacke, U.G., Jacobsen, A.L., Lens, F., Maherali, H., Martínez-Vilalta, J.,
763 Mayr, S., Mencuccini, M., Mitchell, P.J., Nardini, A., Pittermann, J., Pratt, R.B., Sperry, J.S.,
764 Westoby, M., Wright, I.J., Zanne, A.E., 2012. Global convergence in the vulnerability of
765 forests to drought. Nature 491, 752–755. https://doi.org/10.1038/nature11688
766 Cochard, H., 2020. A new mechanism for tree mortality due to drought and heatwaves. bioRxiv
767 531632. https://doi.org/10.1101/531632
768 Cramer III, R.D., Bunce, J.D., Patterson, D.E., Frank, I.E., 1988. Crossvalidation, Bootstrapping,
769 and Partial Least Squares Compared with Multiple Regression in Conventional QSAR
770 Studies. Quant. Struct.-Act. Relatsh. 7, 18–25. https://doi.org/10.1002/qsar.19880070105
771 Cramer, W., Guiot, J., Fader, M., Garrabou, J., Gattuso, J.-P., Iglesias, A., Lange, M.A., Lionello, P.,
772 Llasat, M.C., Paz, S., Peñuelas, J., Snoussi, M., Toreti, A., Tsimplis, M.N., Xoplaki, E., 2018.
773 Climate change and interconnected risks to sustainable development in the Mediterranean.
774 Nat. Clim. Change 8, 972–980. https://doi.org/10.1038/s41558-018-0299-2
775 Das, A.J., Battles, J.J., Stephenson, N.L., van Mantgem, P.J., 2007. The relationship between tree
776 growth patterns and likelihood of mortality: a study of two tree species in the Sierra Nevada.
777 Can. J. For. Res. 37, 580–597. https://doi.org/10.1139/X06-262
778 Davi, H., Cailleret, M., 2017. Assessing drought-driven mortality trees with physiological process-
779 based models. Agric. For. Meteorol. 232, 279–290.
780 https://doi.org/10.1016/j.agrformet.2016.08.019
781 DeSoto, L., Cailleret, M., Sterck, F., Jansen, S., Kramer, K., Robert, E.M.R., Aakala, T., Amoroso,
782 M.M., Bigler, C., Camarero, J.J., Čufar, K., Gea-Izquierdo, G., Gillner, S., Haavik, L.J.,

783 Hereş, A.-M., Kane, J.M., Kharuk, V.I., Kitzberger, T., Klein, T., Levanič, T., Linares, J.C.,
784 Mäkinen, H., Oberhuber, W., Papadopoulos, A., Rohner, B., Sangüesa-Barreda, G.,
785 Stojanovic, D.B., Suárez, M.L., Villalba, R., Martínez-Vilalta, J., 2020. Low growth resilience
786 to drought is related to future mortality risk in trees. Nat. Commun. 11, 545.
787 https://doi.org/10.1038/s41467-020-14300-5
788 DGAL, 2018. Surveillance des dépérissements en forêts. Note de service DGAL/SDQSPV/2018-
789 433.
790 Dobbertin, M., 2005. Tree growth as indicator of tree vitality and of tree reaction to environmental
791 stress: a review. Eur. J. For. Res. 124, 319–333. https://doi.org/10.1007/s10342-005-0085-3
792 Dobbertin, M., Brang, P., 2001. Crown defoliation improves tree mortality models. For. Ecol. Manag.
793 141, 271–284. https://doi.org/10.1016/S0378-1127(00)00335-2
794 Dobbertin, M., Hilker, N., Rebetez, M., Zimmermann, N.E., Wohlgemuth, T., Rigling, A., 2005. The
795 upward shift in altitude of pine mistletoe (Viscum album ssp. austriacum) in Switzerland—the
796 result of climate warming? Int. J. Biometeorol. 50, 40–47. https://doi.org/10.1007/s00484-
797 005-0263-5
798 Dobbertin, M., Rigling, A., 2006. Pine mistletoe (Viscum album ssp. austriacum) contributes to Scots
799 pine (Pinus sylvestris) mortality in the Rhone valley of Switzerland. For. Pathol. 36, 309–322.
800 https://doi.org/10.1111/j.1439-0329.2006.00457.x
801 Eichhorn, J., Roskams, P., Potocic, N., Timmermann, V., Ferretti, M., Mues, V., Szepesi, A.,
802 Durrant, D., Seletkovic, I., Schroeck, H.-W., Nevalainen, S., Bussotti, F., Garcia, P., Wulff,
803 S., 2020. Part IV Visual assessment of crown condition and damaging agents, Thünen
804 Institute of Forest Ecosystems. ed.
805 Fernandes, V., 2012. En quoi l'approche PLS est-elle une méthode a (re)-découvrir pour les
806 chercheurs en management ? M@n@gement 15, 102–123.
807 https://doi.org/10.3917/mana.151.0102
808 Ferretti, M., 2021. New appetite for the monitoring of European forests. Ann. For. Sci. 78, 94.
809 https://doi.org/10.1007/s13595-021-01112-w
810 Franklin, J.F., Shugart, H.H., Harmon, M.E., 1987. Tree Death as an Ecological Process.
811 BioScience 37, 550–556. https://doi.org/10.2307/1310665

812 Galiano, L., Martínez-Vilalta, J., Lloret, F., 2010. Drought-Induced Multifactor Decline of Scots Pine
813 in the Pyrenees and Potential Vegetation Change by the Expansion of Co-occurring Oak
814 Species. Ecosystems 13, 978–991. https://doi.org/10.1007/s10021-010-9368-8
815 Gaudio, N., Balandier, P., Perret, S., Ginisty, C., 2011. Growth of understorey Scots pine (Pinus
816 sylvestris L.) saplings in response to light in mixed temperate forest. For. Int. J. For. Res. 84,
817 187–195. https://doi.org/10.1093/forestry/cpr005
818 Gaylord, M.L., Kolb, T.E., McDowell, N.G., 2015. Mechanisms of piñon pine mortality after severe
819 drought: a retrospective study of mature trees. Tree Physiol. 35, 806–816.
820 https://doi.org/10.1093/treephys/tpv038
821 Gea-Izquierdo, G., Férriz, M., García-Garrido, S., Aguín, O., Elvira-Recuenco, M., Hernandez-
822 Escribano, L., Martin-Benito, D., Raposo, R., 2019. Synergistic abiotic and biotic stressors
823 explain widespread decline of Pinus pinaster in a mixed forest. Sci. Total Environ. 685, 963–
824 975. https://doi.org/10.1016/j.scitotenv.2019.05.378
825 Gessler, A., Cailleret, M., Joseph, J., Schönbeck, L., Schaub, M., Lehmann, M., Treydte, K., Rigling,
826 A., Timofeeva, G., Saurer, M., 2018. Drought induced tree mortality – a tree-ring isotope
827 based conceptual model to assess mechanisms and predispositions. New Phytol. 219, 485–
828 490.
829 Gessler, A., Schaub, M., McDowell, N.G., 2017. The role of nutrients in drought-induced tree
830 mortality and recovery. New Phytol. 214, 513–520. https://doi.org/10.1111/nph.14340
831 Girard, F., Vennetier, M., Guibal, F., Corona, C., Ouarmim, S., Herrero, A., 2012. Pinus halepensis
832 Mill. crown development and fruiting declined with repeated drought in Mediterranean
833 France. Eur. J. For. Res. 131, 919–931. https://doi.org/10.1007/s10342-011-0565-6
834 Gonthier, P., Giordano, L., Nicolotti, G., 2011. Further observations on sudden diebacks of Scots
835 pine in the European Alps. For. Chron. https://doi.org/10.5558/tfc86110-1
836 Goudet, M., Saintonge, F.-X., Nageleisen, L.-M., 2018. Quantifier l'état de santé de la forêt,
837 méthode simplifiée d'évaluation. Dép. Santé For. 1–6.
838 Granier, A., Loustau, D., Bréda, N., 2000. A generic model of forest canopy conductance dependent
839 on climate, soil water availability and leaf area index. Ann. For. Sci. 57, 755–765.
840 https://doi.org/10.1051/forest:2000158

841 Guada, G., Camarero, J.J., Sánchez-Salguero, R., Cerrillo, R.M.N., 2016. Limited Growth Recovery
842 after Drought-Induced Forest Dieback in Very Defoliated Trees of Two Pine Species. Front.
843 Plant Sci. 7. https://doi.org/10.3389/fpls.2016.00418
844 Hartmann, H., Moura, C.F., Anderegg, W.R.L., Ruehr, N.K., Salmon, Y., Allen, C.D., Arndt, S.K.,
845 Breshears, D.D., Davi, H., Galbraith, D., Ruthrof, K.X., Wunder, J., Adams, H.D., Bloemen,
846 J., Cailleret, M., Cobb, R., Gessler, A., Grams, T.E.E., Jansen, S., Kautz, M., Lloret, F.,
847 O'Brien, M., 2018. Research frontiers for improving our understanding of drought-induced
848 tree and forest mortality. New Phytol. 218, 15–28. https://doi.org/10.1111/nph.15048
849 Hawksworth, F.G., Scharpf, R.F., 1986. Spread of European mistletoe (Viscum album) in California,
850 U.S.A. For. Pathol. 16, 1–5. https://doi.org/10.1111/j.1439-0329.1986.tb01045.x
851 Hegyi F. 1974. A simulation model for managing jackpine stands. In: Fries J, Ed. Growth models for
852 tree and stand simulation. Stockholm: Royal College of Forestry. p 74–90.
853 Helama, S., Läänelaid, A., Raisio, J., Mäkelä, H.M., Hilasvuori, E., Jungner, H., Sonninen, E., 2014.
854 Oak decline analyzed using intraannual radial growth indices, δ13C series and climate data
855 from a rural hemiboreal landscape in southwesternmost Finland. Environ. Monit. Assess.
856 186, 4697–4708. https://doi.org/10.1007/s10661-014-3731-8
857 Hoch, G., Toffolo, E.P., Netherer, S., Battisti, A., Schopf, A., 2009. Survival at low temperature of
858 larvae of the pine processionary moth *Thaumetopoea pityocampa* from an area of range
859 expansion. Agric. For. Entomol. 11, 313–320. https://doi.org/10.1111/j.1461-
860 9563.2009.00431.x
861 Hódar, J.A., Castro, J., Zamora, R., 2003. Pine processionary caterpillar Thaumetopoea pityocampa
862 as a new threat for relict Mediterranean Scots pine forests under climatic warming. Biol.
863 Conserv. 110, 123–129. https://doi.org/10.1016/S0006-3207(02)00183-0
864 Holzwarth, F., Kahl, A., Bauhus, J., Wirth, C., 2013. Many ways to die – partitioning tree mortality
865 dynamics in a near-natural mixed deciduous forest. J. Ecol. 101, 220–230.
866 https://doi.org/10.1111/1365-2745.12015
867 Hosmer, J., Lemeshow, S., Sturdivant, R.X., 2013. Applied Logistic Regression. John Wiley & Sons.

868 Hülsmann, L., Bugmann, H., Cailleret, M., Brang, P., 2018. How to kill a tree: empirical mortality
869 models for 18 species and their performance in a dynamic forest model. Ecol. Appl. 28, 522–
870 540. https://doi.org/10.1002/eap.1668
871 Iversen, J., 1944. Viscum, Hedera and Ilex as Climate Indicators. Geol. Fören. Stockh. Förh. 66,
872 463–483. https://doi.org/10.1080/11035894409445689
873 Jamagne, M., Bétrémieux, R., Bégon, J.C., Mori, A., 1977. Quelques données sur la variabilité dans
874 le milieu naturel de la réserve en eau des sols. Bull. Tech. Inf. 324–325, 627–641.
875 Jeffree, C.E., Jeffree, E.P., 1996. Redistribution of the Potential Geographical Ranges of Mistletoe
876 and Colorado Beetle in Europe in Response to the Temperature Component of Climate
877 Change. Funct. Ecol. 10, 562–577. https://doi.org/10.2307/2390166
878 Joly, D., Brossard, T., Cardot, H., Cavailhes, J., Hilal, M., Wavresky, P., 2010. Les types de climats
879 en France, une construction spatiale. Cybergeo Eur. J. Geogr.
880 https://doi.org/10.4000/cybergeo.23155
881 Julio Camarero, J., Gazol, A., Sangüesa-Barreda, G., Cantero, A., Sánchez-Salguero, R., Sánchez-
882 Miranda, A., Granda, E., Serra-Maluquer, X., Ibáñez, R., 2018. Forest Growth Responses to
883 Drought at Short- and Long-Term Scales in Spain: Squeezing the Stress Memory from Tree
884 Rings. Front. Ecol. Evol. 6, 9. https://doi.org/10.3389/fevo.2018.00009
885 Kopecký, M., Macek, M., Wild, J., 2021. Topographic Wetness Index calculation guidelines based
886 on measured soil moisture and plant species composition. Sci. Total Environ. 757, 143785.
887 https://doi.org/10.1016/j.scitotenv.2020.143785
888 Larsson, J., 2021. Eulerr: Area-proportional Euler and Venn diagrams with ellipses. R Package
889 Version 6.1.0, 2020, https://cran.r-project.org/package=eulerr.
890 Le Houerou, H.N., 2005. The Isoclimatic Mediterranean Biomes : Bioclimatology, Diversity and
891 Phytogeography . Volume I et II, Montpellier, Copymania Publication. ed.
892 Lieutier, F., Faure, T., Garcia, J., 1988. Lieutier F. et al, 1988. Les attaques de scolytes et le
893 dépérissement du pin sylvestre dans la région PACA. RFF XL – 3 - 1988. Rev. For. Fr. XL,
894 224–232.

895 Linares, J.C., Camarero, J.J., 2012. Growth patterns and sensitivity to climate predict silver fir
896 decline in the Spanish Pyrenees. Eur. J. For. Res. 131, 1001–1012.
897 https://doi.org/10.1007/s10342-011-0572-7
898 Lloret, F., Keeling, E.G., Sala, A., 2011. Components of tree resilience: effects of successive low-
899 growth episodes in old ponderosa pine forests. Oikos 120, 1909–1920.
900 https://doi.org/10.1111/j.1600-0706.2011.19372.x
901 Manion, P.D., 1991. Tree disease concepts. Prentice Hall, Englewood Cliffs, N.J.
902 Masson-Delmotte, V., Zhai, P., Pirani, A., Connors, S.L., Péan, C., Chen, Y., Goldfarb, L., Gomis,
903 M.I., Berger, S., Caud, N., Huang, M., Leitzell, K., Lonnoy, E., Matthews, J.B.R., Maycock,
904 T.K., Waterfield, T., Yelekçi, O., Yu, R., Zhou, B., 2021. IPCC, 2021 : Summary for
905 Policymakers. In: Climate Change 2021: The Physical Science Basis. Contribution of
906 Working Group I to the Sixth Assessment Report of the Intergovernmental Panel on Climate
907 Change, Cambridge University Press. In Press. ed.
908 Matías, L., Linares, J.C., Sánchez-Miranda, Á., Jump, A.S., 2017. Contrasting growth forecasts
909 across the geographical range of Scots pine due to altitudinal and latitudinal differences in
910 climatic sensitivity. Glob. Change Biol. 23, 4106–4116. https://doi.org/10.1111/gcb.13627
911 McDowell, N., Pockman, W.T., Allen, C.D., Breshears, D.D., Cobb, N., Kolb, T., Plaut, J., Sperry, J.,
912 West, A., Williams, D.G., Yepez, E.A., 2008. Mechanisms of plant survival and mortality
913 during drought: why do some plants survive while others succumb to drought? New Phytol.
914 178, 719–739. https://doi.org/10.1111/j.1469-8137.2008.02436.x
915 Médail, F., 2001. Biogéographie, écologie et valeur patrimoniale des forêts de pin sylvestre (Pinus
916 sylvestris L.) en région méditerranéenne. For. Méditerranéenne XXII, 5–22.
917 Meinzer, F.C., Woodruff, D.R., Shaw, D.C., 2004. Integrated responses of hydraulic architecture,
918 water and carbon relations of western hemlock to dwarf mistletoe infection. Plant Cell
919 Environ. 27, 937–946. https://doi.org/10.1111/j.1365-3040.2004.01199.x
920 Mellado, A., Zamora, R., 2014. Linking safe sites for recruitment with host-canopy heterogeneity:
921 The case of a parasitic plant, Viscum album subsp. austriacum (Viscaceae). Am. J. Bot. 101,
922 957–964. https://doi.org/10.3732/ajb.1400096

923 Monserud, R.A., 1976. Simulation of Forest Tree Mortality. For. Sci. 22, 438–444.
924 https://doi.org/10.1093/forestscience/22.4.438
925 Morcillo, L., Gallego, D., González, E., Vilagrosa, A., 2019. Forest Decline Triggered by Phloem
926 Parasitism-Related Biotic Factors in Aleppo Pine (Pinus halepensis). Forests 10, 608.
927 https://doi.org/10.3390/f10080608
928 Müller, E., Stierlin, H.R., 1990. Sanasilva Tree crown photos., Sanasilva. ed, Swiss Federal Institute
929 for Forest, Snow and Landscape Research, Birmensdorf.
930 Mutlu, S., Osma, E., Ilhan, V., Turkoglu, H.I., Atici, O., 2016. Mistletoe (Viscum album) reduces the
931 growth of the Scots pine by accumulating essential nutrient elements in its structure as a
932 trap. Trees 30, 815–824. https://doi.org/10.1007/s00468-015-1323-z
933 Odland, A., 2009. Interpretation of altitudinal gradients in South Central Norway based on vascular
934 plants as environmental indicators. Ecol. Indic. 9, 409–421.
935 https://doi.org/10.1016/j.ecolind.2008.05.012
936 Oliva, J., Stenlid, J., Grönkvist-Wichmann, L., Wahlström, K., Jonsson, M., Drobyshev, I.,
937 Stenström, E., 2016. Pathogen-induced defoliation of Pinus sylvestris leads to tree decline
938 and death from secondary biotic factors. For. Ecol. Manag. 379, 273–280.
939 https://doi.org/10.1016/j.foreco.2016.08.011
940 Paulo, J.A., Palma, J.H.N., Gomes, A.A., Faias, S.P., Tomé, J., Tomé, M., 2015. Predicting site
941 index from climate and soil variables for cork oak (Quercus suber L.) stands in Portugal.
942 New For. 46, 293–307. https://doi.org/10.1007/s11056-014-9462-4
943 Pauly, H., Belrose, V., 2005. La santé des forêts françaises: actualités de l'année 2004 -
944 Sécheresse et canicule de l'été 2003: observation en 2004 des conséquences sur les
945 peuplements forestiers adultes. Rapp. Ministère L'Agriculture L'Alimentation Pêche Rural.
946 Dép. Santé For. Paris P 11.
947 Pedersen, B.S., 1998. The Role of Stress in the Mortality of Midwestern Oaks as Indicated by
948 Growth Prior to Death. Ecology 79, 79–93. https://doi.org/10.1890/0012-
949 9658(1998)079[0079:TROSIT]2.0.CO;2

950 Petroselli, A., Vessella, F., Cavagnuolo, L., Piovesan, G., Schirone, B., 2013. Ecological behavior of
951 Quercus suber and Quercus ilex inferred by topographic wetness index (TWI). Trees 27,
952 1201–1215. https://doi.org/10.1007/s00468-013-0869-x
953 Piedallu, C., Gégout, J.C., 2007. Multiscale computation of solar radiation for predictive vegetation
954 modelling. Ann. Sci. For. 64, 899–909.
955 Poyatos, R., Aguadé, D., Galiano, L., Mencuccini, M., Martínez-Vilalta, J., 2013. Drought-induced
956 defoliation and long periods of near-zero gas exchange play a key role in accentuating
957 metabolic decline of Scots pine. New Phytol. 200, 388–401.
958 https://doi.org/10.1111/nph.12278
959 Quintana-Seguí, P., Moigne, P.L., Durand, Y., Martin, E., Habets, F., Baillon, M., Canellas, C.,
960 Franchisteguy, L., Morel, S., 2008. Analysis of Near-Surface Atmospheric Variables:
961 Validation of the SAFRAN Analysis over France. J. Appl. Meteorol. Climatol. 47, 92–107.
962 https://doi.org/10.1175/2007JAMC1636.1
963 Raduła, M.W., Szymura, T.H., Szymura, M., 2018. Topographic wetness index explains soil
964 moisture better than bioindication with Ellenberg's indicator values. Ecol. Indic. 85, 172–179.
965 https://doi.org/10.1016/j.ecolind.2017.10.011
966 Ramsauer, J., Brotons, L., Herrando, S., Morán-Ordóñez, A., 2021. A multi-scale landscape
967 approach to understand dispersal of the mistletoe by birds in Mediterranean pine forests.
968 Landsc. Ecol. https://doi.org/10.1007/s10980-021-01369-6
969 Rathgeber, C.B.K., Misson, L., Nicault, A., Guiot, J., 2005. Bioclimatic model of tree radial growth:
970 application to the French Mediterranean Aleppo pine forests. Trees 19, 162–176.
971 https://doi.org/10.1007/s00468-004-0378-z
972 Rigling, A., Bigler, C., Eilmann, B., Feldmeyer-Christe, E., Gimmi, U., Ginzler, C., Graf, U., Mayer,
973 P., Vacchiano, G., Weber, P., Wohlgemuth, T., Zweifel, R., Dobbertin, M., 2013. Driving
974 factors of a vegetation shift from Scots pine to pubescent oak in dry Alpine forests. Glob.
975 Change Biol. 19, 229–240. https://doi.org/10.1111/gcb.12038
976 Rigling, A., Eilmann, B., Koechli, R., Dobbertin, M., 2010. Mistletoe-induced crown degradation in
977 Scots pine in a xeric environment. Tree Physiol. 30, 845–852.
978 https://doi.org/10.1093/treephys/tpq038

Robinet, C., Baier, P., Pennerstorfer, J., Schopf, A., Roques, A., 2007. Modelling the effects of climate change on the potential feeding activity of Thaumetopoea pityocampa (Den. & Schiff.) (Lep., Notodontidae) in France. Glob. Ecol. Biogeogr. 16, 460–471. https://doi.org/10.1111/j.1466-8238.2006.00302.x

Robinet, C., Rousselet, J., Roques, A., 2014a. Potential spread of the pine processionary moth in France: preliminary results from a simulation model and future challenges. Ann. For. Sci. 2 71 149-160 2014.

Robinet, C., Rousselet, J., Roques, A., 2014b. Potential spread of the pine processionary moth in France: preliminary results from a simulation model and future challenges. Ann. For. Sci. 71, 149–160. https://doi.org/10.1007/s13595-013-0287-7

RStudio Team, 2021. RStudio: Integrated Development Environment for R. RStudio, PBC, Boston, MA URL http://www.rstudio.com/.

Santini, F., Ferrio, J.P., Hereş, A.-M., Notivol, E., Piqué, M., Serrano, L., Shestakova, T.A., Sin, E., Vericat, P., Voltas, J., 2018. Scarce population genetic differentiation but substantial spatiotemporal phenotypic variation of water-use efficiency in Pinus sylvestris at its western distribution range. Eur. J. For. Res. 137, 863–878. https://doi.org/10.1007/s10342-018-1145-9

Sardin, T., 1997. La sylviculture des boisements de protection, la problématique de leur renouvellement. For. Méditerranéenne XVIII, 232–237.

Schütt, P., Cowling, E.B., 1985. Waldsterben, a general decline of forests in central Europe: symptoms, development and possible causes. Plant Dis. 69, 548–558.

Sergent, A.-S., 2011. Diversité de la réponse au déficit hydrique et vulnérabilité au dépérissement du douglas (These de doctorat). Orléans.

Shaw, D.C., Lee, C.A., 2020. Expansion of the invasive European mistletoe in California, USA. Botany 98, 517–524. https://doi.org/10.1139/cjb-2019-0215

Skre, O., 1979. The regional distribution of vascular plants in Scandinavia with requirements for high summer temperatures. Nor. J. Bot. 295–318.

Solomon, N.U., James, I.M., Alphonsus, N.O.-O., Nkiruka, R.U., 2015. A Review of Host-Parasite Relationships. Annu. Res. Rev. Biol. 372–384. https://doi.org/10.9734/ARRB/2015/10263

1008 Stastny, M., Battisti, A., Petrucco-Toffolo, E., Schlyter, F., Larsson, S., 2006. Host-plant use in the
1009 range expansion of the pine processionary moth, Thaumetopoea pityocampa. Ecol. Entomol.
1010 31, 481–490. https://doi.org/10.1111/j.1365-2311.2006.00807.x
1011 Suarez, M.L., Ghermandi, L., Kitzberger, T., 2004. Factors predisposing episodic drought-induced
1012 tree mortality in Nothofagus– site, climatic sensitivity and growth trends. J. Ecol. 92, 954–
1013 966. https://doi.org/10.1111/j.1365-2745.2004.00941.x
1014 Taccoen, A., Piedallu, C., Seynave, I., Gégout-Petit, A., Nageleisen, L.-M., Bréda, N., Gégout, J.-C.,
1015 2021. Climate change impact on tree mortality differs with tree social status. For. Ecol.
1016 Manag. 489, 119048. https://doi.org/10.1016/j.foreco.2021.119048
1017 Taccoen, A., Piedallu, C., Seynave, I., Perez, V., Gégout-Petit, A., Nageleisen, L.-M., Bontemps, J.-
1018 D., Gégout, J.-C., 2019. Background mortality drivers of European tree species: climate
1019 change matters. Proc. R. Soc. B Biol. Sci. 286, 20190386.
1020 https://doi.org/10.1098/rspb.2019.0386
1021 Tenenhaus, M., 1998. La régression PLS: théorie et pratique. Editions TECHNIP.
1022 Ter-Braak, C.J.T., Juggins, 1993. Weighted averaging partial least square regression (WA-PLS): an
1023 improved method for reconstructing environnemental variables from species assemblages.
1024 Hydrobiologia 269–270, 485-502.
1025 Teskey, R., Wertin, T., Bauweraerts, I., Ameye, M., Mcguire, M.A., Steppe, K., 2015. Responses of
1026 tree species to heat waves and extreme heat events. Plant Cell Environ. 38, 1699–1712.
1027 https://doi.org/10.1111/pce.12417
1028 Thabeet, A., 2008. Réponse du pin sylvestre (Pinus sylvestris L) aux changements climatiques
1029 récents en région méditerranéenne française : spatialisation et quantification par la
1030 télédétection et la dendrochronologie (These de doctorat). Aix-Marseille 3.
1031 Thabeet, A., Vennetier, M., Gadbin-Henry, C., Denelle, N., Roux, M., Caraglio, Y., Vila, B., 2009.
1032 Response of Pinus sylvestris L. to recent climatic events in the French Mediterranean
1033 region. Trees 23, 843–853. https://doi.org/10.1007/s00468-009-0326-z
1034 Trugman, A.T., Anderegg, L.D.L., Anderegg, W.R.L., Das, A.J., Stephenson, N.L., 2021. Why is
1035 Tree Drought Mortality so Hard to Predict? Trends Ecol. Evol. 0.
1036 https://doi.org/10.1016/j.tree.2021.02.001

1037 Trugman, A.T., Detto, M., Bartlett, M.K., Medvigy, D., Anderegg, W.R.L., Schwalm, C., Schaffer, B.,
1038 Pacala, S.W., 2018. Tree carbon allocation explains forest drought-kill and recovery
1039 patterns. Ecol. Lett. 21, 1552–1560. https://doi.org/10.1111/ele.13136
1040 Turc, L., 1955. Le bilan d'eau des sols. Relations entre les précipitations, l'évaporation et
1041 l'écoulement. Annales Agronomiques 6:5.
1042 Vennetier et al, 2007. Impact of climate change on pine forest productivity and on the shift of a
1043 bioclimatic limit in a Mediterranean area. Options Méditerranéennes Série A 75, 189–197.
1044 Vennetier, M., Girard, F., Cailleret, M., Taugourdeau, O., Caraglio, Y., Sabatier, A.-S., Ouarmim, S.,
1045 Thabeet, A., 2013. Climate change impact on tree architectural development and leaf area.
1046 Climate change: Realities, impacts over ice cap, sea level and risks. pp. 103–126.
1047 Vennetier, M., Ripert, C., Maille, E., Blanc, L., Torre, F., Roche, P., Tatoni, T., Brun, J.J., 2008. A
1048 new bioclimatic model calibrated with flora for Mediterranean forested areas. Ann. For. Sci.
1049 65, 12.
1050 Vennetier, M., Ripert, C., Rathgeber, C., 2018. Autecology and growth of Aleppo pine (Pinus
1051 halepensis Mill.): A comprehensive study in France. For. Ecol. Manag. 413, 32–47.
1052 https://doi.org/10.1016/j.foreco.2018.01.028
1053 Venturas, M.D., Todd, H.N., Trugman, A.T., Anderegg, W.R.L., 2021. Understanding and predicting
1054 forest mortality in the western United States using long-term forest inventory data and
1055 modeled hydraulic damage. New Phytol. 230, 1896–1910. https://doi.org/10.1111/nph.17043
1056 Vogel, J., Paton, E., Aich, V., Bronstert, A., 2021. Increasing compound warm spells and droughts in
1057 the Mediterranean Basin. Weather Clim. Extrem. 32, 100312.
1058 https://doi.org/10.1016/j.wace.2021.100312
1059 Wang, A., Lehmann, M.M., Rigling, A., Gessler, A., Saurer, M., Du, Z., Li, M.-H., 2022. There Is No
1060 Carbon Transfer Between Scots Pine and Pine Mistletoe but the Assimilation Capacity of the
1061 Hemiparasite Is Constrained by Host Water Use Under Dry Conditions. Front. Plant Sci. 13.
1062 Waring, R.H., 1987. Characteristics of Trees Predisposed to Die. BioScience 37, 569–574.
1063 https://doi.org/10.2307/1310667

Weiss, A.D., 2001. Topographic position and landforms analysis. ESRI User Conférence “The Nature Conservancy” (San Diego, Californie). Poster URL Httpwwwjennessentcomdownloadstpi-Poster-Tnc18x22pdf.

Zuber, D., 2004. Biological flora of Central Europe: Viscum album L. Flora - Morphol. Distrib. Funct. Ecol. Plants 199, 181–203. https://doi.org/10.1078/0367-2530-00147

Zweifel, R., Bangerter, S., Rigling, A., Sterck, F.J., 2012. Pine and mistletoes: how to live with a leak in the water flow and storage system? J. Exp. Bot. 63, 2565–2578. https://doi.org/10.1093/jxb/err432

8. Appendices

Appendix A. List of variables used in the different dieback models

Type of variable	Variable	Unit	Scale	Period	Number of variables	Description	Source
Target variables Y	FolDef	%	tree	2017	1	Foliar deficit of the tree microphylls included	Field measurement
	XStem50	%	plot	2017	1	Percentage of stems per plot with at least 50% leaf loss and/or branching	
	DECL_XSTEM_th	0 or 1	plot	2017	3	Number of plots with Xstem50 above a given threshold (th = 20%, 25%, 30%)	
Biotic factors	%CrownVa	%	tree	2017	1	Percentage of crown colonized by mistletoe	Field measurement
	NbNestTp	nb	tree	2017	1	Number of nests per tree on the plot	Field measurement
	G_Tot	m^2/ha	plot	2017	1	Basal area	Field measurement
	DBHm	cm	tree	2017	1	Mean diameter of *Pinus sylvestris* at breast height	Field measurement
	Hmean	m	tree	2017	1	Mean height of *Pinus sylvestris*	Field measurement
	Age	years	tree	2017	1	Age of the tree	laboratory measurement
	DBHt	cm	tree	2017	1	Diameter of the tree *t* at breast height (130 cm)	Field measurement
	DBHt/DBHp	/	tree	2017	1	Ratio of DBHt to the mean diameter of the trees growing in the same plot *p*	Field measurement
	Gs	mm^2/y	tree		1	Mean annual basal area increment	laboratory measurement
	Gs20	mm^2/y	tree	1997-2016	1	Mean annual basal area increment for the last 20 years	laboratory measurement
	Gsb	mm^2/y	tree	1997-2002	1	Mean annual basal area increment before the major climatic stress	laboratory measurement
	Gsd	mm^2/y	tree	2003-2007	1	Mean annual basal area increment during the major climatic stress	laboratory measurement
	Gsa	mm^2/y	tree	2008-2016	1	Mean annual basal area increment after the major climatic stress	laboratory measurement
	RS	/	tree		1	Resistance, ratio GSd/GSb	laboratory measurement
	RC	/	tree		1	Recovery, ratio Gsa/Gsd	laboratory measurement
	RE	/	tree		1	Resilience, ratio Gsa/Gsb	laboratory measurement
	PPI_caterpillar_r	ha	plot	2014	9	Area covered by pine species (*P. sylvestris, P. halepensis, P. nigra ssp nigra, P. nigra ssp laricio*) susceptible to the caterpillar (*Thaumetopoea pityocampa*) within different radius (*r*) around the center of the study plot (*r* = 500 m, 1 km, 2 km, 4 km, 6 km, 8 km, 16 km, 32 km, 64 km)	Database of French national land survey IGN
	PPI_mistletoe_r	ha	plot	2014	9	Area covered by pine species (*P. sylvestris, P. nigra ssp nigra, P. nigra ssp laricio*) susceptible to mistletoe (*Viscum album sp austriacum*) within different radius (*r*) around the center of the study plot (*r* = 500 m, 1 km, 2 km, 4 km, 6 km, 8 km, 16 km, 32 km, 64 km)	
Climatic factors	Tmean_m	°C	plot	1981-2010	12	Mean monthly temperature for the months January (m=1) to December (m=12)	Climatic model AURELHY © METEOFRANCE (precipitation and temperature)
	Tmean_year	°C	plot	1981-2010	1	Mean annual temperature	
	Tmean_1202	°C	plot	1981-2010	1	Mean winter temperature (December to February)	
	Tmean_0608	°C	plot	1981-2010	1	Mean summer temperature (from June to August)	
	TX_6-8	°C	plot	1981-2010	1	Mean of the maximum temperature 1981-2010 from June to August	
	TN_m	°C	plot	1981-2010	6	Mean of the minimum temperature for the months October (m=10) to March (m=3)	
	TN_1003	°C	plot	1981-2010	1	Mean of the maximum temperature 1981-2010 from October to March	
	P_year	mm	plot	1981-2010	1	Mean annual precipitation	
	P_0608	mm	plot	1981-2010	1	Precipitation 1981-2010 from June to August	
	P_0509	mm	plot	1981-2010	1	Precipitation 1981-2010 from May to September	
	P_0410	mm	plot	1981-2010	1	Precipitation 1981-2010 from April to October	
	P_1103	mm	plot	1981-2010	1	Precipitation 1981-2010 from November to March	
	PET_m	mm	plot	1981-2010	12	Potential evapotranspiration (Turc Formula) for the months January (m=1) to December (m=12)	
	PET_1003	mm	plot	1981-2010	1	Potential evapotranspiration (Turc Formula) 1981-2010 October to March	
	PET_1004	mm	plot	1981-2010	1	Potential evapotranspiration (Turc Formula) 1981-2010 October to April	
	PET_0410	mm	plot	1981-2010	1	Potential evapotranspiration (Turc Formula) 1981-2010 October to April	
	PET_0509	mm	plot	1981-2010	1	Potential evapotranspiration (Turc Formula) 1981-2010 May to September	
	PET_0608	mm	plot	1981-2010	1	Potential evapotranspiration (Turc Formula) 1981-2010 June to August	
	PET_year	mm	plot	1981-2010	1	Annual potential evapotranspiration (Turc formula) 1981-2010	
	PET_1103	mm	plot	1981-2010	1	Potential evapotranspiration (Turc formula) 1981-2010 November to March	
	P-PET_0608	mm	plot	1981-2010	1	Climatic water balance (P-PET) 1981-2010 June to August	
	P-PET_0509	mm	plot	1981-2010	1	Climatic water balance (P-PET) 1981-2010 May to September	
	P-PET_0410	mm	plot	1981-2010	1	Climatic water balance (P-PET) 1981-2010 April to October	
	P-PET_1103	mm	plot	1981-2010	1	Climatic water balance (P-PET) 1981-2010 November to March	
	P-ETP_year	mm	plot	1981-2010	1	Annual climatic water balance (P-PET) 1981-2010	
	ray_year	J/cm^2	plot	1971-2000	1	Sum of annual radiation 1971-2000	DIGITALIS © AGROPARISTECH model
	TNABS	°C	plot	1981-2010	1	lowest temperature recorded each year during the 1981-2010 period	Climatic model SAFRAN © METEOFRANCE See 2.3.2 and Lemaire and Pigeon 2015
	SKRE_I	/	plot	1981-2010	1	Skre index	See Equation 1 section 2.4 (Skre 1979, Dobbertin 2005)
Soil and topographic factors	TEI	/	plot			Topoedaphic index Appendix A *	Field measurement
	Elevation	m	plot	-	1	Elevation	DEM IGN 25 m resolution
	TPI_100	/	plot	-	1	Topographic position index in a radius of 100 m around the center of the plot	DEM IGN 25 m resolution
	TPI_1500	/	plot	-	1	Topographic position index in a radius of 1500 m around the center of the plot	DEM IGN 75 m resolution
	IKR	/	plot	-	1	Radiation index of Becker 1982	Field measurement
	pH_Hz_Ah	/	plot	-	1	pH groundwater at 20 cm depth	Field measurement
	TWI	/	plot	-	1	Topographic wetness index	DEM IGN 75 m resolution
						**All the variables necessary to calculate the TEI (Appendix 1) were also measured*	

Appendix B. Temporal change in basal area increment of healthy and declining trees

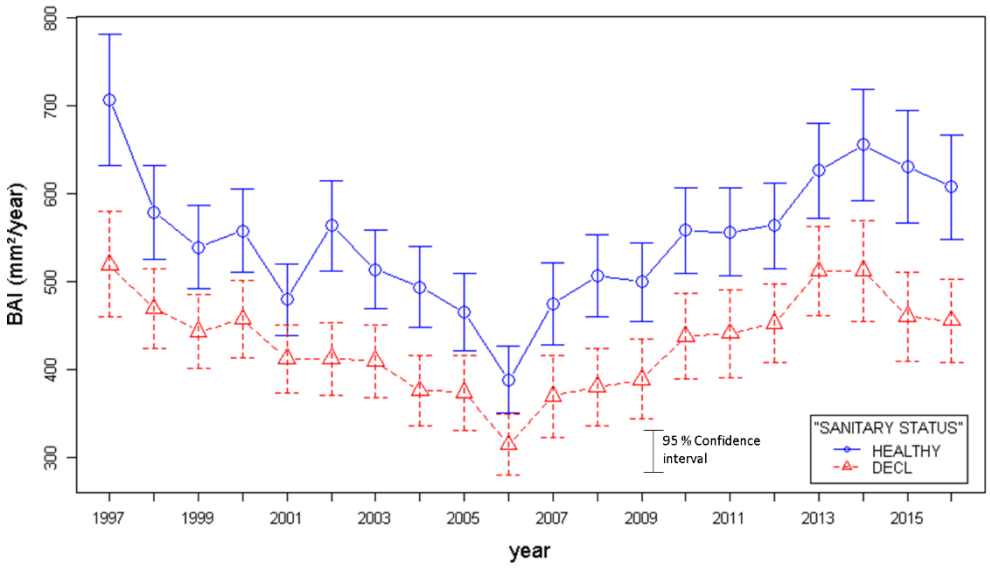

Figure B1. Temporal change in mean basal area increment of healthy (HEALTHY) and declining (DECL) trees

Appendix C. Effect of the sub-sampling on the development of the stand dieback model

To develop the foliar deficit model at tree scale, which includes annual radial growth data from cores, a subsample of 28 plots was selected among the 87 plots of the study, covering all the stratification classes (see 2.2 in main text).

The absence of bias arising from subsampling was checked to ensure that this subsample of 28 plots (FolDef: mean = 51.8%, SD = 13.1%) was representative of the whole set of 87 plots (FolDef: mean = 48.3%, SD = 11.7%).

In this way, we compared the stand dieback models constructed over the whole set of 87 plots (see Table 1 in the main text) with this same dieback model calibrated on those 28 plots. The significant variables retained in the two models were the same, and their non-standardized coefficients were not significantly different (Figure B1).

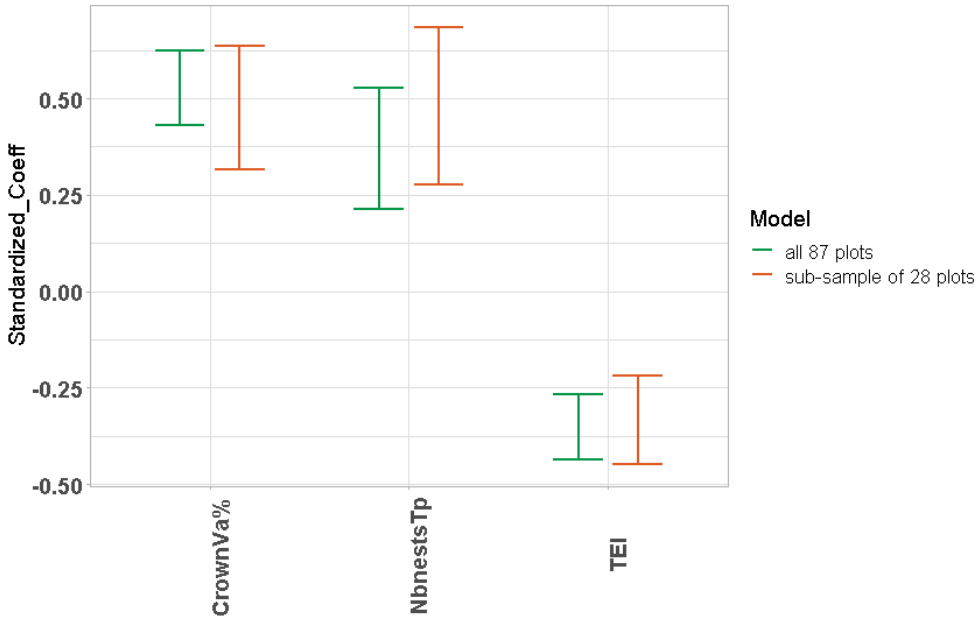

Figure C1. 95% confidence interval of centered values (standardized coefficients) of significant variables for the stand dieback model constructed over the whole set of 87 plots (DECL_STAND) and for the subsample of 28 plots (SUB-SAMPLE).CrownVa is the percentage of pine crowns colonized by mistletoe per plot (%); NbnestTp is the number of processionary moth nests per plot; TEI is the field-based topoedaphic index.

Appendix D. Estimation of the Topoedaphic index TEI

		UNFAVORABLE FACTORS						NEUTRAL FACTORS		FAVORABLE FACTORS			
Landform	General topography	Convex ridges, peaks and higher slopes	-14	Regular top of slope	-6	Regular slope	-3	plateau	0	Concave lower slope	10	Valley, thalweg bottom	18
	Plot scale topography			convex	-8			Flat	0	concave	8		
	Former farmland Terraces							absence	0	presence	13		
	Slope angle					≥50%	-1	<50%	0				
Rock	Rock outcrop (%)	≥30%	-8	]10-30%]	-3	[1-10%]	-1	0%	0				
	Stone cover at soil surface (%)			≥30	-3	[10-30%[	-2	[1-10%[	0	0	2		
	Dip angle vs slope					unfavorable	-1	neutral	0	favorable	1		
	Joints and cracks through rock layers (per m)					<5	-2	5-15	0	> 15	3		
Material	Reference material	Mother rock	-4	alterite	-2	lapiaz	-1			colluvium	5		
	Earth reaction to HCl					strong	-2	weak	0	none	3		
	Hard rocks coarse fragments in soil	≥90%	-7	[60-90%[	-3			[30-60%[	0	<30%	4		
	Horizontal imbricated alterite plates			presence	-6			absence	0				
	Fine earth Water Holding Capacity (mm/cm)*	≤ 0.7	-10	]0.7-1.3]	-3			]1.3-1.6]	0	]1.6-1.95]	2	>1.95	10
Depth	Colluvium thickness (cm)			absence	-2	[5-20]	-1	[25-50]	0	>50	3		
	total depth (cm)	[0-22.5[	-12	[22.5-47.5[	-5			[47.5-75[	0	[75-100]	5	>100	10
	Mean depth 5 auger tests (cm)					[0-20]	-2	]20-40]	0	]40-75]	2	>75	3
Topoedaphic Index (TEI)		=		+		+		+		+		+	

Table D1. Description of the determination of the topoedaphic index (TEI) according to field-based topography, bedrock, soil material, and soil depth variables. The plot TEI is obtained by adding the coefficients (grey columns) corresponding to each variable. More details are available in Vennetier et al. (2018), especially concerning the relationship between Water Holding Capacity and fine earth texture.

Appendix E. Choice of Xstem50 threshold

Three thresholds in Xstem50 were tested during the development of the risk model corresponding to values published in the literature: 20% (DGAL, 2018), 25 % (Linares and Camarero, 2012), and 30% (Brunier *et al*., 2020).

Based on comparisons of the confusion matrix and the AUC, the threshold that best discriminated stands with and without dieback was 30% (Table D1).

XSTEM50%	AIC	Misclassed on 87 plots	Chi2_Pearson	RSS	R^2Y	AUC	Error rate
20%							
Nb_Comp_1	88.79	**24**	70.86	14.24	**0.30**	**0.830**	**27.6%**
25%							
Nb_Comp_1	77.6	**21**	71.23	12.28	**0.43**	**0.877**	**24.1%**
30%							
Nb_Comp_1	77.48	**19**	73.53	12.11	**0.44**	**0.882**	**21.8%**

Table E1. Comparison of the performance of the risk models with different Xstem50 thresholds. AIC is the Akaike Information Criterion, RS the residual sum of squares, R^2Y the coefficient of determination, AUC the Area Under the receiver operating characteristics Curve.

Appendix F. Tree age and DBH distribution

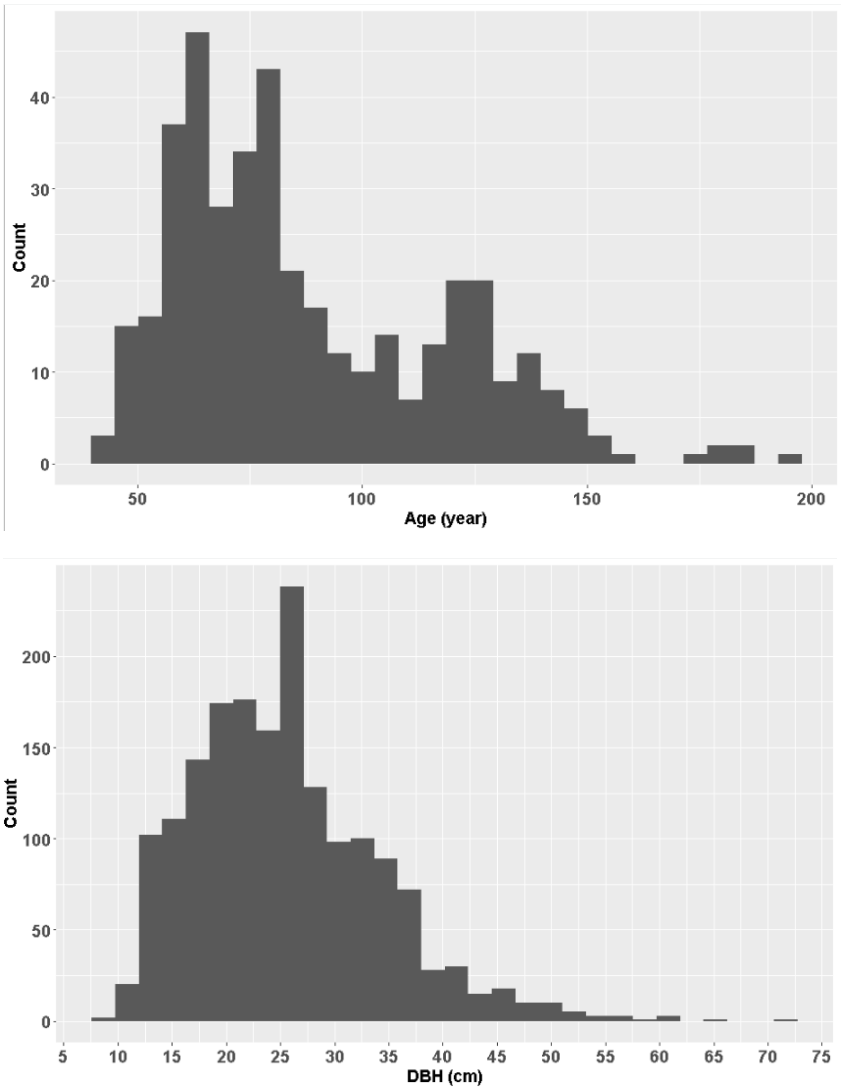

Figure F1. Distribution in age of the trees cored (n = 402; *Left*) and in diameter at breast height (DBH) of all trees measured (n = 1440; *Right*).

Appendix G. Abundance of mistletoe and pine processionary moth

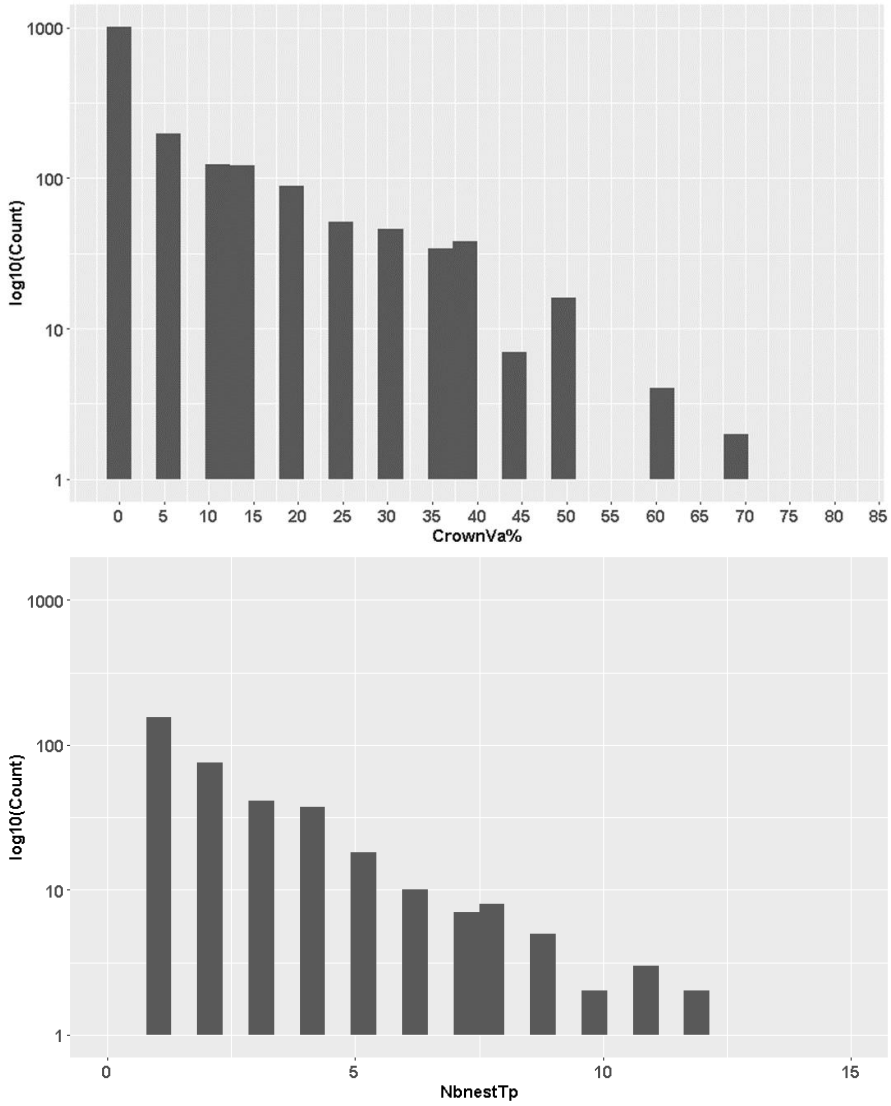

Figure G1. Distribution of percentage of crown colonized by mistletoe (CrownVa%) measured and pine processionary moth nests (NbnestTp) for 1740 trees

Appendix H. Differences in mean foliar deficit among stratification classes

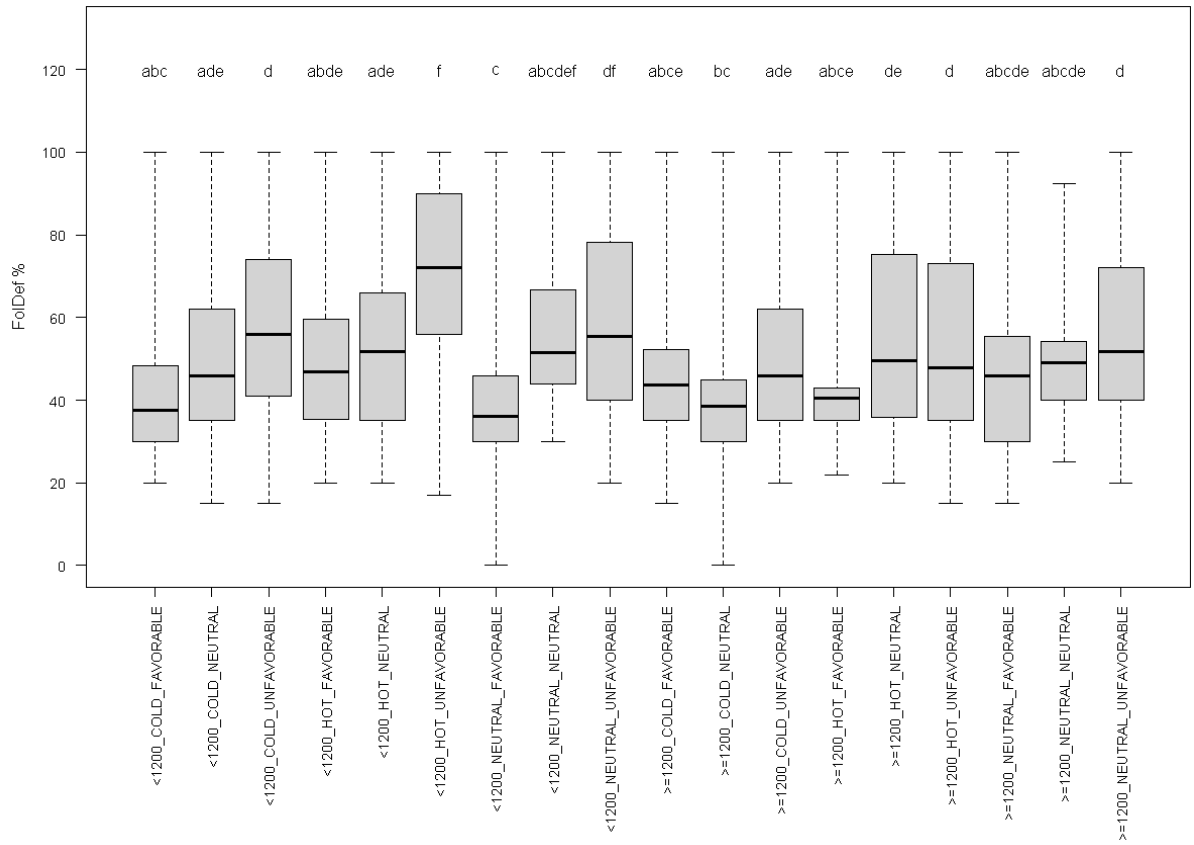

Figure H1. Differences in tree foliar deficit (FolDef, %) between each combination of class of elevation (<1200m; >=1200m), IKR (HOT, NEUTRAL, COLD) and topoedaphic index (TEI; FAVORABLE, NEUTRAL, UNFAVORABLE). Rectangles delimit two central quartiles separated by the median. Groups sharing the same letter did not differ significantly (Nemeyi test; $p < 0.05$).